Geological and geophysical study of a thin-skinned tectonic wedge formed in an early collisional stage: The Outer Tuscan Nappe (Northern Apennines, Italy)

Outer Tuscan Nappe: a fossil fold-and-thrust belt

Category: **Structural Geology**

Filippo Carboni[1], Francesco Brozzetti[2], Francesco Mirabella[1], Francesco Cruciani[3], Massimiliano Porreca[1], Maurizio Ercoli[1], Stefan Back[4] & Massimiliano R. Barchi[1]

[1] GSG, Dipartimento di Fisica e Geologia, Università degli Studi di Perugia, Via Alessandro Pascoli, 06123, Perugia.

[2] CRUST, Università degli Studi "G. d'Annunzio" Chieti-Pescara, Via dei Vestini, 66013, Chieti.

[3] Formerly at Università degli Studi di Perugia, now at ENI S.p.A.

[4] Geologisches Institut, RWTH Aachen University, Wüllnerstr. 252056, Aachen.

*Corresponding author (e-mail: filippocarboni@ymail.com)

Abstract. The presence of a set of well-known turbidite successions, deposited in progressively east-migrating foredeep basins, subsequently piled up with east vergence, makes the Northern Apennines of Italy paradigmatic of the evolution of deepwater fold-and-thrust belts (DWFTBs). This study focuses on the early Apenninic collisional stage, early Miocene in age, which led to the accretion of the turbidites of the Outer Tuscan Nappe (OTN). Based on the interpretation of previously unpublished seismic reflection profiles with new surface-geology data and tectonic balancing, we present a detailed tectonic reconstruction of the OTN of the central part of the

Northern Apennines (Italy). In the study area, the OTN is characterized by a west-dipping shaly basal décollement located at a depth of 1 to 5 km. The tectonic wedge is about 5 km thick in its central-western part and tapers progressively eastward to about 1 km. Total shortening, balanced along a 33 km long cross section, is about 60 km, including 20 km (40%) of internal imbrication, about 23 km of horizontal ENE-ward translation along the basal décollement, and ~ 17 km of passive translation caused by the later shortening of footwall units. Deformation balancing, constrained through biostratigraphy to the late Aquitanian–late Burdigalian (ca. 21–16 Ma), provides an average shortening rate of ~ 8.6 mm/yr. Internal shortening of the OTN shows, for this period, an average shortening rate of ~ 4 mm/yr.

Key words: Foreland fold-and-thrust belt; Thin-skinned tectonics; Seismic reflection profiles; Northern Apennines, Italy.

1. Introduction

During the evolution of a convergent plate boundary, different types of fold-and-thrust belts (FTBs) are generated, i.e. accretionary prisms and foreland FTBs (e.g. Price, 1981; Moore & Silver, 1987; Poblet & Lisle, 2011 and references therein). In the early collision stage, the toe of the deforming thrust wedge is fully submarine; the associated deepwater sedimentary record is classically termed flysch (Allen *et al*. 1991; Sinclair, 1997). As the foreland basin becomes filled with sediment, depositional environments become shallow marine and continental; these sediments are classically termed molasse (e.g. Sinclair, 1997; Allen *et al.* 2001; Allen & Allen, 2005). In the inner part of mature FTBs, tectonic units related to the early contractional stages can often be recognized. These units were emplaced during the early deepwater stage of collision or possibly during the accretionary prism stage.

A prime example for the complex, time-dependent tectonic-stratigraphic evolution of FTBs is the Northern Apennine belt of Italy (Fig. 1).

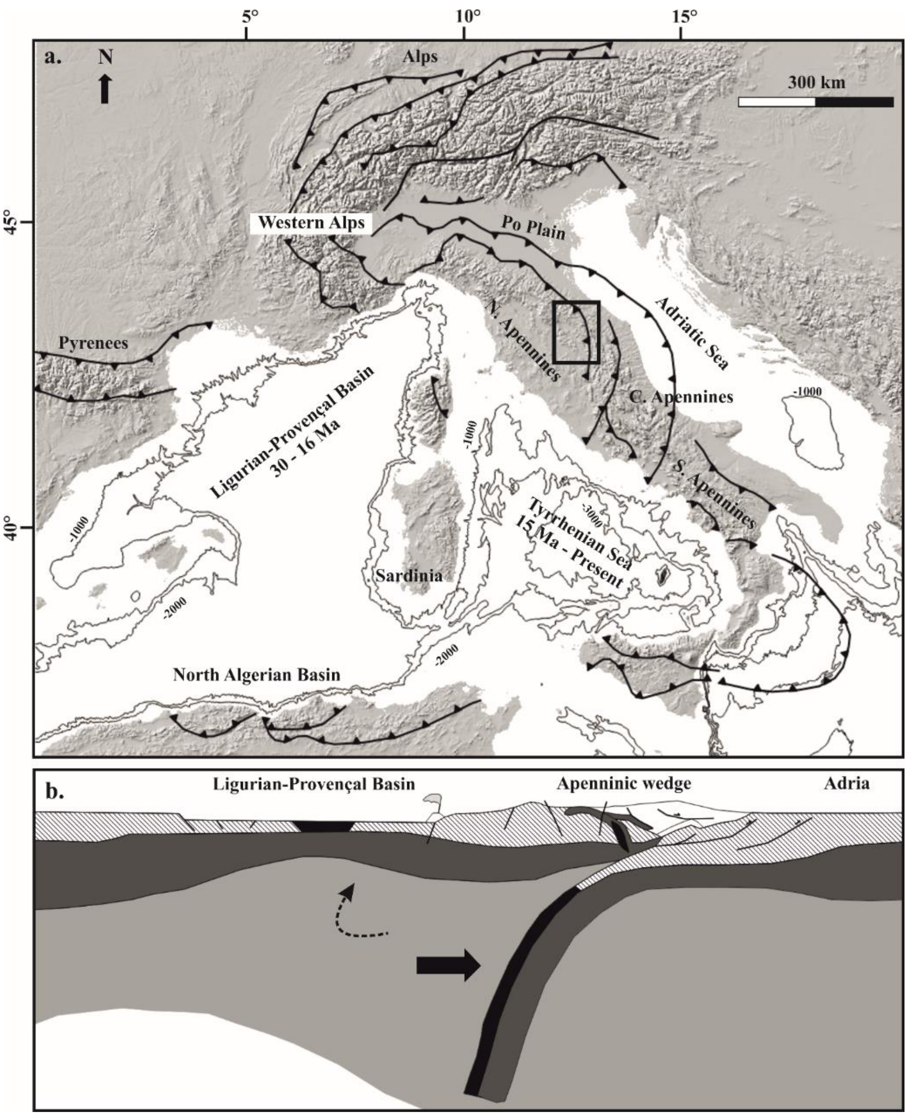

Fig. 1. (a) tectonic setting of the peri-Mediterranean region including the main mountain belts and basins. (b) section showing the middle Miocene beginning of retreat of the Apenninic subduction zone with transtension in Corsica and Northern Tyrrhenian sea. (modified after Molli, 2008).

The Northern Apennine belt is presently an emerged FTB, associated with a shallow marine (Northern Adriatic) and a continental (Po Plain) molasse-type foreland basin. The external front of the Northern Apennine FTB is still active, as demonstrated by the presence of compressional seismicity (e.g. Boccaletti *et al.* 2010; Ponza *et al*. 2010; Gunderson *et al.* 2013; Maesano *et al*. 2013; Chiarabba *et al.* 2014; Maesano *et al*. 2015; Martelli *et al.* 2017; Maestrelli *et al*. 2018) as well as by geodetic GPS data (Hunstad *et al.* 2003; Serpelloni *et al.* 2005, 2006; Bennett *et al.*

2012; Devoti *et al.* 2017). Within the inner and central parts of the Northern Apennines, diachronous syn-orogenic successions were deposited in eastward-migrating foreland basins, and emplaced in-sequence either during the accretionary prism stage or during the subsequent early and mature stages of continental collision (e.g. Merla, 1951; Ricci Lucchi, 1986; Barchi *et al.* 2001).

This paper focuses on the Tuscan Nappe (Fig. 2), a complex stack of transported (i.e. allochthonous) tectonic units, originally pertaining to the same paleo-geographic (Tuscan) domain, in the inner portion of the Northern Apennine FTB (e.g. Carmignani *et al*. 2001).

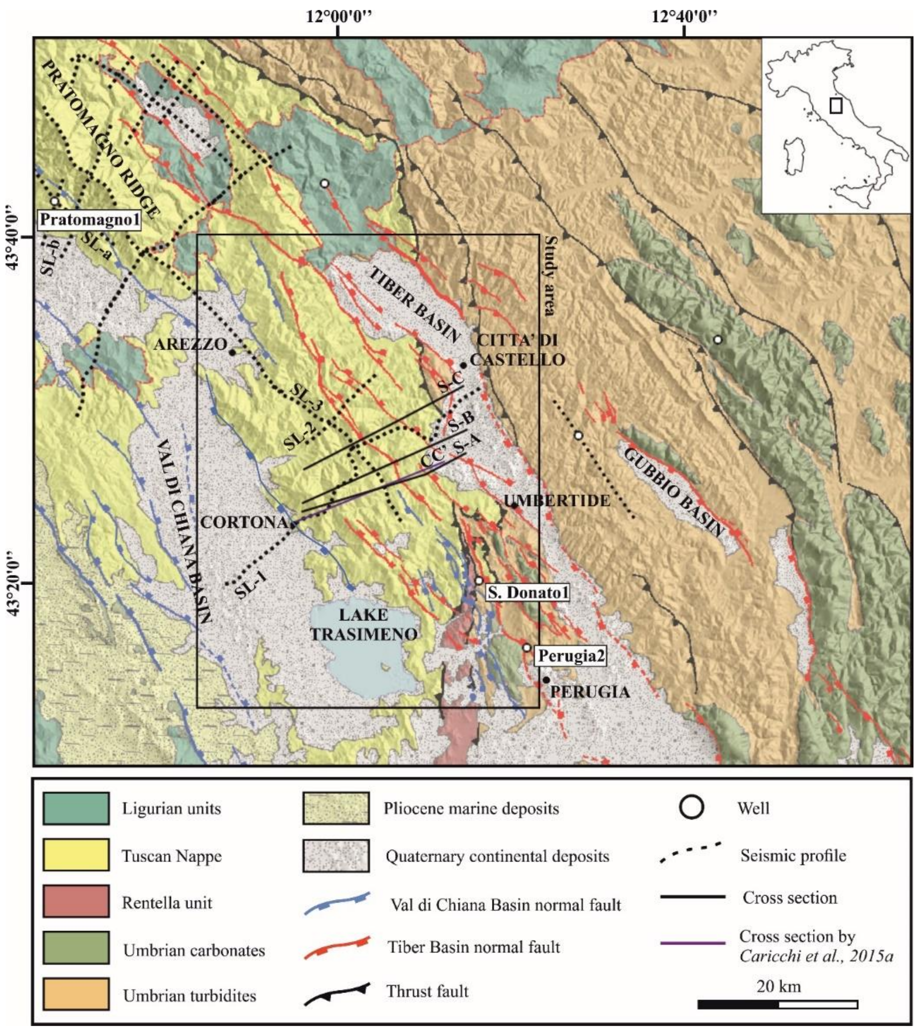

Fig. 2. Regional geological scheme reporting the relative position of the stacked units, the main thrusts and normal faults traces, basins, outcropping units, geological cross sections, wells, and seismic traces displayed. Normal faults have two colours: the blue ones are related to the Val di Chiana Basin, the red ones to the High Tiber Basin. (modified after Mirabella *et al*. 2011).

The Tuscan Nappe can be subdivided based on its present-day position into an Inner Tuscan Nappe (e.g., Monte Amiata area; Brogi *et al*. 2015) and the Outer Tuscan Nappe (OTN) in the study area north of Trasimeno Lake (Fig. 2). The study area is bounded by two major Pliocene-Quaternary extensional basins, the Val di Chiana Basin to the West and the High Tiber Basin to the East (Fig. 2).

The OTN is an early Miocene imbricate thrust complex comprising Late Cretaceous-Tertiary rocks. Due to well-exposed outcrops, the stratigraphy and tectonics of the OTN were intensively studied in the past by many researchers (e.g. Nocchi, 1961, 1962; Baldacci *et al*. 1967; Sestini, 1970; Ricci Lucchi, 1986; Abbate & Bruni, 1987; Costa *et al.* 1991, 1997; Damiani *et al*. 1991; D'Offizi *et al.* 1994; Aruta & Pandeli, 1995; Brozzetti *et al.* 2000, 2002; Plesi *et al.* 2002*a*, *b*; Brozzetti, 2007; Barsella *et al.* 2009). In recent time, the knowledge of the OTN was significantly increased by several studies, comprising: i) the publication of new 1:50.000 geological maps, in the framework of the CARG (CARtografia Geologica) project (sheets 289, 299 and 310 of the Carta Geologica d'Italia; Pialli *et al.* 2009; Barchi *et al.* 2010; Plesi *et al.* 2010); ii) geo-thermometric measures, aimed at defining the wedge thickness and the amount of post-orogenic erosion (Thomson *et al*. 2010; Meneghini *et al.* 2012; Caricchi *et al.* 2015*a*, *b*) and iii) a paleomagnetic campaign, constraining vertical axes rotation of the OTN (Caricchi *et al.* 2014).

In this study, the subsurface structure of the OTN is investigated by the interpretation of a previously unpublished set of 2D seismic reflection profiles acquired in the 1980's for hydrocarbon exploration purposes, calibrated by deep borehole data from the Pratomagno1 well (see locations in Fig. 2). These data, combined with existing surface geology knowledge, provide a comprehensive view of the stratigraphy, internal architecture and tectonic evolution of the OTN. The overall geometry of the thrust complex is synthesized along a 33 km long, WSW-ENE oriented integrated geological cross-section, extrapolated down to about 9 km depth; the kinematic evolution of the tectonic wedge is investigated by a 2D restoration of the integrated section.

The results of this tectonic interpretation and restoration study contribute to a better understanding of the OTN by documenting and discussing: i) the original wedge geometry before it was uplifted and deeply eroded, and partly dissected by later extensional tectonics; ii) the total amount of shortening and the kinematic relationship between the basal décollement and the internal imbrication; and iii) the mechanics of the wedge.

The tectonic balancing of the OTN provides, within the uncertainty limits, a comprehensive image of the geometry of the Northern Apennines during the early Miocene early continental collision stage. The reconstruction results can be thus – in a wider perspective – compared to data collected in modern DWFTBs worldwide, formed under similar geodynamic conditions. Since the fossil OTN is located onshore and in places well exposed, it forms a paradigmatic field analogue for modern DWFTBs.

2. The Northern Apennines (regional and geodynamic framework)

The Northern Apennines form an orogenic belt, that is the backbone of the northern part of the Italian peninsula between the Western Alps and the Central/Southern Apennines (Fig. 1). The tectonic evolution and the geodynamic scenario of the Northern Apennines are complex and controversial in the literature (e.g. Jolivet *et al.* 1998; Doglioni *et al.* 1999; Lavecchia *et al.* 2003; Molli, 2008 and references therein). Following Molli (2008) and Molli & Malavieille (2011), the Northern Apennines evolution can be schematically divided into two major stages, with opposite subduction polarity: the first stage (“Alpine Cycle”, Late Cretaceous–middle Eocene) is characterized by an east-dipping intraoceanic and then continental subduction of the European-Corsica Plate; the second stage (“Apenninic Cycle”, Oligocene to present) is characterized by a west-dipping subduction of the remnant oceanic lithosphere of the late Mesozoic Western Tethys Ocean (i.e. the late Mesozoic ocean separating paleo-Europe and paleo-Africa plates) and of the attached, thinned continental crust of Adria. The westward retreat of the subducting Adria Plate generated the back-arc extension of the Ligurian-Provençal Basin (Oligocene–early Miocene) and, subsequently, back-arc extension of the Tyrrhenian Basin (middle Miocene to present). During the "Apenninic Cycle", i.e. since the Oligocene, the eastward migration of the orogen is marked by the eastward progressively younger age of the foredeep and the occurrence of piggy-back basin deposits, which were subsequently incorporated into the Northern Apennines FTB (e.g. Merla, 1951; Ori *et al.* 1986; Ricci Lucchi, 1986; Barchi *et al.* 2001; Casero, 2004).

The Northern Apennines comprise a stack of imbricate tectonic units derived from the Mesozoic Tethys Ocean (Ligurian domain) and the adjacent continental passive margin of Adria (Tuscan and Umbria-Marche-Romagna domains) (Fig. 2). Recent reviews of the stratigraphy, structural setting, and evolution of the Northern Apennines are provided by Carmignani *et al.* (2001) and Molli *et al.* (2010) for the inner Tuscan region, and by Barchi *et al.* (2001) and Barchi (2010) for the outer Umbria-Marche region.

In the study area (Fig. 2), stratigraphic successions pertaining to all the main paleo-geographic domains of the Northern Apennines are exposed, with the individual stratigraphy shown in Figure 3. The Ligurian Domain is here represented by a pre-orogenic succession, consisting of narrow outcrops of ophiolites and their sedimentary cover including Upper Jurassic–Lower Cretaceous pelagites, covered by syn-orogenic Upper Cretaceous–lower Tertiary turbidites (Barchi *et al.* 2010). The Tuscan Domain (Plesi *et al.* 2002*b*; Barsella *et al.* 2009) includes a pre-orogenic Mesozoic–Paleogene carbonate multilayer and a syn-orogenic succession made up of Eocene–lower Oligocene marly limestones of the Scaglia Toscana Fm., overlain by the siliciclastic foredeep turbidites of the Macigno Fm. (Chattian–Aquitanian) (Plesi *et al.* 2002*b*; Barsella *et al.* 2009).

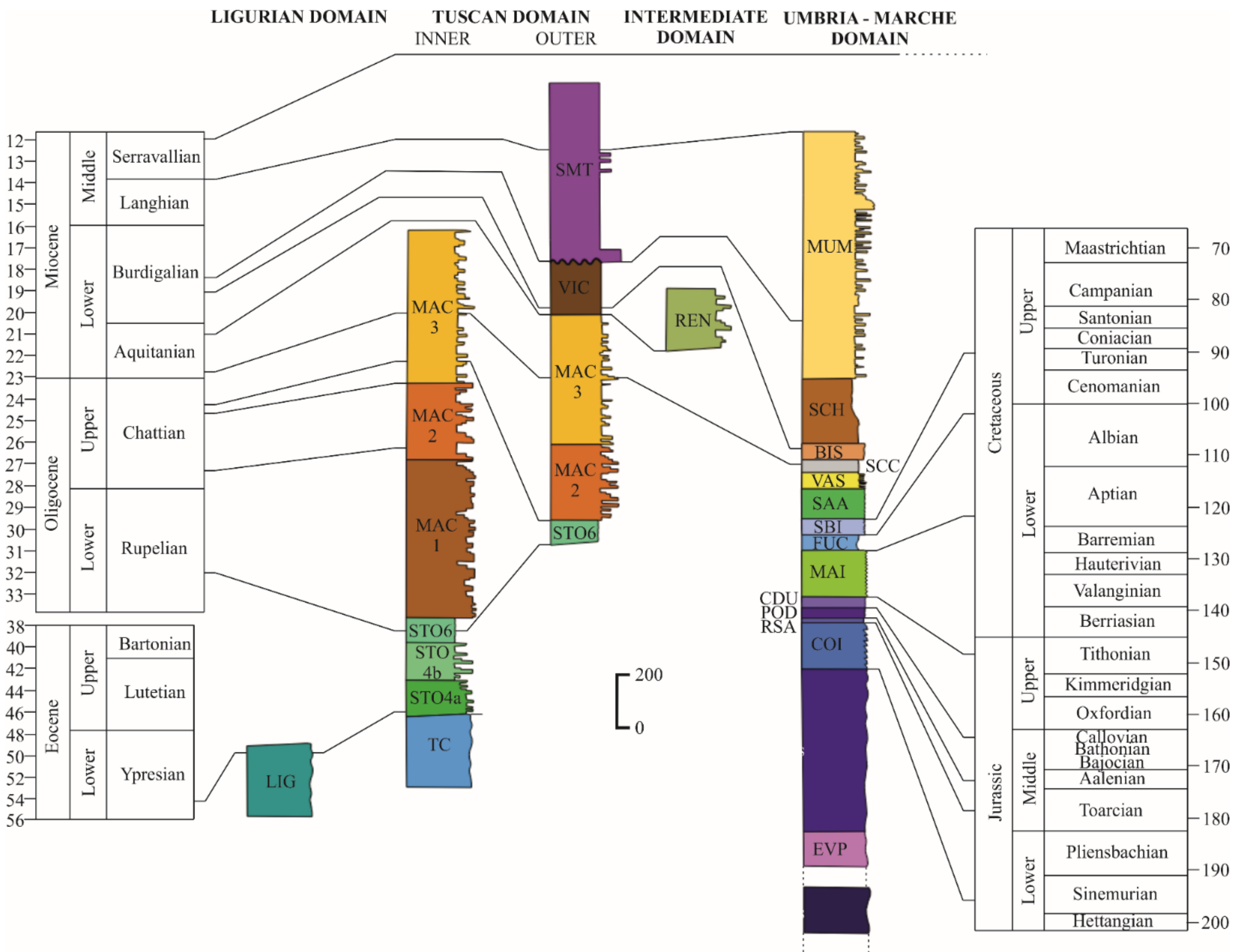

Fig. 3. Chronostratigraphic log representing the relative position of the stacked units, timing of deposition and thickness. LIG: Ligurian units; SMT: Santa Maria Tiberina Fm.; VIC: Marne di Vicchio Fm.; MAC: members of the Macigno Formation; TSC: members of the Scaglia Toscana Fm.; TC: Tuscan Carbonates; REN: Rentella intermediate unit; MUM: Marnoso-Arenacea Fm.; SCH: Schlier Fm.; BIS: Bisciaro Fm.; SCC: Scaglia Cinerea Fm.; VAS: Scaglia Variegata Fm.; SAA: Scaglia Rossa Fm.; SBI: Scaglia Bianca Fm.; FUC: Marne a Fucoidi Fm.; MAI: Maiolica Fm.; CDU: Calcari Diasprigni Fm.; POD: Calcari e Marne a Posidonia Fm.; RSA: Rosso Ammonitico Fm.; COI: Corniola Fm.; MAS: Calcare Massiccio Fm.; EVP: Evaporites; BAS: Phyllitic basement.

These deposits are in turn partially covered by the Marne di Vicchio Formation deposited in an upper Aquitanian–middle Burdigalian piggy-back basin. The Umbria-Marche Domain is characterized by a pre-orogenic Mesozoic–Paleogene carbonate multilayer resting on Upper Triassic evaporites, cropping out in the Perugia Mountains (Fig. 2). A basal upper Paleozoic–Middle Triassic metasedimentary succession, drilled in the S. Donato 1 and Perugia 2 wells, is also documented (Martinis & Pieri, 1964; Menichetti & Minelli, 1991; Anelli *et al.* 1994). The calcareous multilayer is overlain by the syn-orogenic lower-middle Miocene foredeep turbidites of the Marnoso-Arenacea Fm. (e.g. Brozzetti *et al*. 2002; Pialli *et al.* 2009; Plesi *et al.* 2010). The Rentella Intermediate Domain, is located in the southernmost part of the study area, between the Tuscan (to the west) and the Umbria-Marche (to the east) domains. It consists of syn-orogenic Rupelian–Aquitanian varicoloured pelagic and hemipelagic marls, topped by Aquitanian–Burdigalian siliciclastic foredeep turbidites (Signorini & Alimenti, 1968; Brozzetti *et al.* 2000; Barsella *et al.* 2009).

Since the late Miocene, eastward migrating extensional tectonics in the western part of the Northern Apennines dissected the previous compressional structures (Barchi, 2010 and references therein), a process which is still active in the main ridge of the Apennines as demonstrated by present-day seismicity (Lavecchia *et al.* 1994; Chiaraluce *et al.* 2017; Porreca *et al.* 2018).

The gross lithology encountered in the OTN provides a clear indication of the deepwater environment in which it developed, and the stratigraphic data effectively constrain the timing of deformation. The sedimentation of the Macigno Fm. occurred in a basin, mostly referred to as being characterized by lower shelf and abyssal plain environments, the latter possibly below the CCD (Monaco & Trecci, 2014). This view is in line with the interpretation of overlying siliceous pelites of the Marne di Vicchio Fm. as draping muds of a middle to deep bathyal environment

(1500 m and 2000 m b.s.l.), deposited in piggy-back basins (Delle Rose *et al.* 1994; Lucchetti *et al.* 2002). In the easternmost position, the emplacement of the OTN along the west boundary of the Umbria foredeep (Marnoso-Arenacea Fm., early–middle Burdigalian), was accompanied by the syn-kinematic deposition of the Monte Santa Maria Tiberina Fm. (late Burdigalian–Serravallian). This formation is recognized to seal the leading edge of the OTN (Brozzetti, 2007), providing a strict temporal constraint for the end of the OTN emplacement, which can be bracketed between late Aquitanian (end of the Macigno Fm. deposition) and the late Burdigalian (initial deposition of the Monte Santa Maria Tiberina Fm.).

3. Surface geology of the study area

Recent geological maps (1:50.000 scale) by the Italian Geological Survey (Pialli *et al.* 2009; Barchi *et al.* 2010; Plesi *et al.* 2010) provide a homogeneous and up-to-date data set for the surface geology of the study area. Through the compilation of these maps, integrated with further structural data collected at selected sites, we produced a synthetic tectonic sketch of the study area (Fig. 4a), and constructed a set of three closely spaced, WSW-ENE trending geological cross-sections (Fig. 4b).

At the surface, the OTN is characterized by a set of eight, major WSW-dipping imbricate thrust faults (T1 to T7, Fig. 4a), each extending several tens of kilometres along strike. The innermost thrust fault (T1) is mostly buried by Pliocene-Quaternary deposits of the Val di Chiana Basin. The thrust fault T6' represents a secondary thrust within the tectonic unit 6, while the thrust fault T5 is divided into 2 major splays (T5a and T5b).

The geological sections (Fig. 4b) show that only the uppermost part (Late Cretaceous–early Miocene) of the Tuscan Domain succession is incorporated in the tectonic units, detached from their original Triassic–Early Cretaceous substrate, whose closest outcrop is located west of the Val di Chiana Basin (Fig. 2; e.g., Damiani *et al.* 1991).

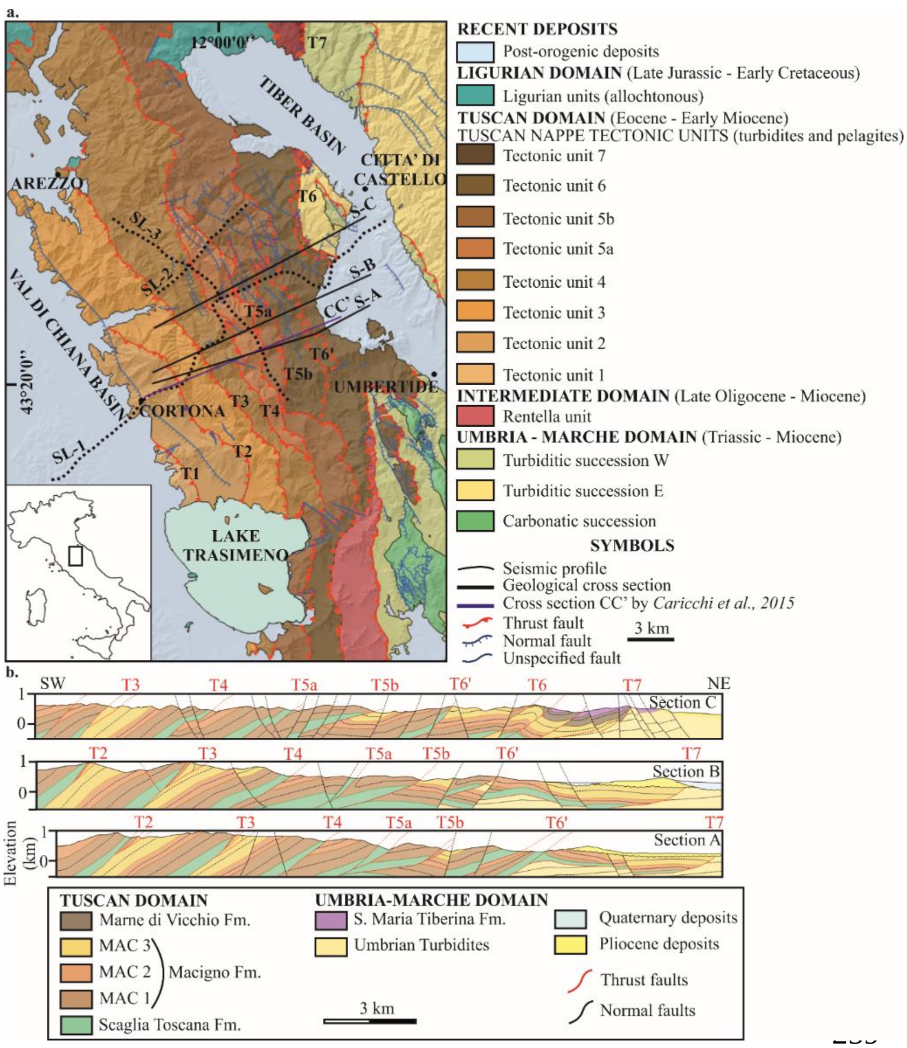

Fig. 4. (a) geological and structural framework of the study area, representing only the main compressive features and structural units of the OTN, the main interpreted seismic lines, the three geological cross sections and the cross section by Caricchi *et al.* 2015*a*. (b) The three geological cross sections positioned from south (Section A) to north (Section C). Both the structural map and the geological sections are based on the 1:50,000 maps produced in the framework of the CARG project (Sheets # 289, 299 and 310 of the Carta Geologica d'Italia (Pialli *et al*. 2009; Plesi *et al*. 2009; Barchi *et al*. 2010).

The internal stratigraphy of the tectonic units (Fig. 3) includes the Scaglia Toscana Fm. and the subsequent Macigno Fm. (subdivided in three members MAC_1, MAC_2 and MAC_3), showing an overall evolution from inner turbidite fan to distal foredeep facies (Plesi *et al.* 2002*b*). The thickness of the Tuscan Domain succession decreases eastward, from the innermost to the outermost units (Fig. 3). The Scaglia Toscana Fm. becomes thinner and comprises only its upper part, due to the eastward up-section trajectory of the basal thrust and a regional-scale pinch out. The Macigno Fm. also becomes thinner eastward and only the two upper members (MAC_2 and

MAC_3) are present in the easternmost tectonic units due to a regional-scale onlap of the turbidites above the late Oligocene foreland ramp (Barsella *et al.* 2009).

The geological sections also show that the major W-dipping thrust faults are accompanied by a set of asymmetric fault-propagation folds, in their hanging wall, involving the three members of the Macigno Fm. Within the OTN tectonic wedge, a systematic decrease in the average splay dip angles can be observed from W to E; along geological cross section B the values range from 27° (T2) to 9° (T6). This suggests that the internal imbrication of the OTN was chiefly characterized by in-sequence thrust propagation, where the emplacement of the younger splays progressively increased the deformation on their hanging wall, thus making the older splays steeper (Boyer & Elliott, 1982).

The tectonic wedge is disrupted by numerous W-dipping and E-dipping normal faults. Extensional tectonics is particularly intense at the western border of the study area, where a major W-dipping normal fault controls the eastern flank of the Val di Chiana Basin (Figs. 2, 4a). Significant extension also occurs in the eastern part of the sections (Fig. 4b), where conjugate, both east-dipping and west-dipping normal faults are observed, locally causing several hundred meters of displacement.

4. Subsurface data

4.a. The seismic data-set

The subsurface dataset used for this project covers an area located between the Pratomagno Ridge, to the North, and the Trasimeno Lake, to the South (see location map in Fig. 2). It consists of i) three seismic reflection profiles (SL-1, SL-2 and SL-3) located in the study area and calibrated with surface geology data, ii) two 2D seismic profiles (SL-a and SL-b) located outside of the study area and iii) the Pratomagno1 well, located about 40 km NW of the SL-2 profile (Fig. 2). All seismic data is in the time domain and were acquired during exploration campaigns carried out between 1975 and 1990.

The interpretation of the most important reflectors of the considered profiles was calibrated with the 4320 m deep Pratomagno1 well (Fig. 5b) (VIDEPI, www.videpi.com), with the well stratigraphy projected onto the closest seismic profiles SL-a and SL-b (traces in Fig. 2).

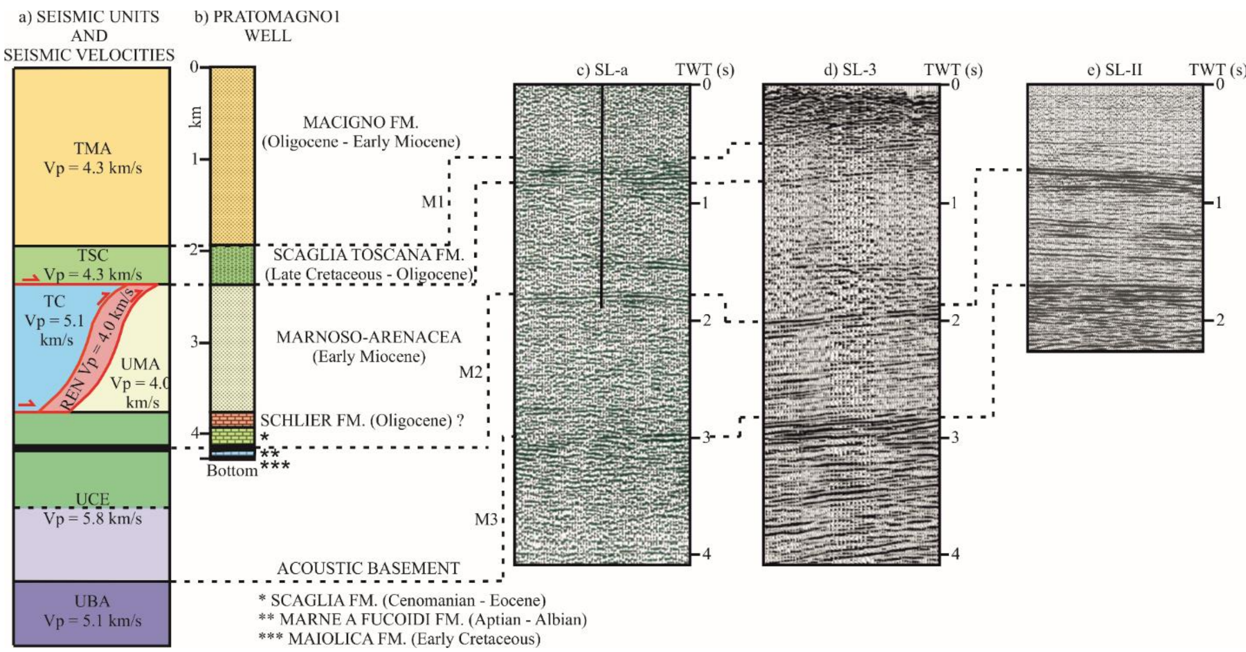

Fig. 5. (a) seismic units with their seismic velocities from Bally et al. 1986 and Mirabella et al. 2011. (b) shows the stratigraphy of the Pratomagno1 well. (c) corresponding reflectors in the seismic profile SL-a. (d) corresponding reflectors in the seismic profile SL-3. (e) corresponding reflectors in the seismic profiles in the seismic profile SL-II.

The stratigraphy of the Pratomagno1 well consists of two superposed tectonic units, i.e., the Tuscan tectonic unit (above) and the Umbria-Marche tectonic unit (below) (Figs. 5a, b). The Tuscan tectonic unit comprises the turbidites of the Macigno Fm. and the underlying Eocene–upper Oligocene Scaglia Toscana Fm., whose base, i.e. the tectonic contact between the two units, is encountered at a depth of 2350 m from the well top. The Umbria-Marche tectonic unit comprises the Umbrian turbidites of the lower–middle Miocene Marnoso-Arenacea Fm., overlying the

Meso–Cenozoic Umbria Carbonates. The base of the well reaches the Lower Cretaceous pelagic limestones of Maiolica Fm., underlying the marly Marne a Fucoidi Fm., intercepted at a depth of 4100 m from the well top.

As demonstrated by previous seismic studies in this region (e.g. Bally *et al.* 1986; Barchi *et al.* 1998*a, b, c*), the Marne a Fucoidi Fm. and the Scaglia Toscana Fm. form the most prominent reflectors in the seismic stratigraphy of the study area, due to their marly lithology that produces a strong acoustic impedance contrast with respect to the adjacent, mainly carbonate rocks. In seismic profile SL-a (Fig. 5c), the Scaglia Toscana Fm. is interpreted to correspond to a group of high-amplitude, medium continuity reflectors between 0.5 s (top) and 0.7 s (base) (TWT). The Marne a Fucoidi Fm., in turn, is a regionally recognized prominent reflector located in the uppermost part (0.1–0.15 s -TWT- below the top) of the Umbrian Carbonates: in seismic profile SL-a (Fig. 5c) it is interpreted on a high-amplitude and laterally continuous reflector at around 1.5 s (TWT). In summary, the Pratomagno1 well provides direct evidence of the superposition of the allochthonous Tuscan tectonic unit over the autochthonous Umbrian-Marche tectonic unit and constrains the main basal thrust, separating the two superposed units, at a depth larger than 2 km. This tectonic stacking is not limited to the study area, but is a regional feature, as demonstrated by other wells in the Northern Apennines (e.g. Suviana1, Anelli *et al.* 1994), that drilled through the Tuscan Nappe into the Umbria-Marche tectonic unit.

We analysed and interpreted in detail the three seismic reflection profiles that cross both transversally (SW-NE, SL-1 and SL-2) and longitudinally (NW-SE, SL-3) the tectonic units of the study area (Fig. 2). SL-1 crosses the entire OTN wedge, SL-2 crosses the study area 4 km North of SL-1, and SL-3 is oriented NW-SE, intercepting both the SL-1 and SL-2 transversal lines.

The three seismic profiles were recorded by using different parameters (e.g., sample rate and record length) and sources (vibroseis or dynamite); a summary of the main acquisition parameters is reported in Table 1.

NAME	SL-1	SL-2	SL-3
SHOT DATE	1982	1987	1976
ORIENTATION	WSW-ENE	WSW-ESE	NNW-SSE
LENGTH (km)	46.7	12.2	19.6
RECORD LENGTH (s)	10	7	6
SAMPLE RATE (ms)	4	2	2
SOURCE	Vibroseis	Dynamite	Dynamite
GEOPHONES TYPE	SM-4 (14Hz)	SM-4 (10Hz)	unknown (14H
SUBSURFACE COVERAGE (%)	1200	1200	600
DATUM (m)	500	500	500

Table 1. Acquisition parameters of the main interpreted seismic lines

The profiles recorded with an explosive source provide a better signal-to-noise ratio and therefore a clearer imaging of the main reflectors. Considering the target units of this study, we limited the interpretation to a depth of around 4 s (TWT); the deepest part of the profiles is characterized by lower quality in terms of resolution and signal-to-noise ratio.

4.b. Seismic stratigraphy

The seismic stratigraphy of the study area, illustrated in Figure 5a, consists of seven seismic units and three major seismic markers, which are described from top to bottom.

Seismic unit TMA (T = Tuscan tectonic unit; MA = Macigno Fm.) is characterized by low-amplitude and high-frequency reflections, generally with low continuity; this unit corresponds to the Macigno Fm. and its thickness varies from 1.5 s and 0.2 s (TWT), thinning north-eastward.

Seismic unit TSC (T = Tuscan tectonic unit; SC = Scaglia Toscana Fm.) is characterized by a series of high-amplitude, low-frequency reflectors, around 0.2 s (TWT) thick; this unit is located below TMA and it is associated with the Scaglia Toscana Fm.

Seismic unit UMA (U = Umbrian tectonic unit; MA = Marnoso-Arenacea Fm.) contains discontinuous, high-amplitude, mid-frequency reflectors and several secondary reflectors slightly dipping south-westward; the observed thickness is generally around 0.6 s (TWT) but, in correspondence with the major thrust faults, it is locally doubled, reaching a thickness of around 1.2 s (TWT). It is associated with the Marnoso-Arenacea Fm..

Seismic unit UCE (U = Umbrian tectonic unit; CE = Carbonates and Evaporites) shows a good continuity, high-amplitude and mid-frequency, the top of this seismic unit is recognized by a couple of near-parallel strong reflectors and its thickness is around 0.9 s (TWT), often increased by a series of deep-seated thrust. This is interpreted as corresponding to the Umbrian Carbonates and Evaporites.

The lowermost seismic unit UBA (U = Umbrian tectonic unit; BA = basement) is composed by high-amplitude, low-frequency reflectors, associated with the acoustic basement of the Umbria-Marche Domain (*sensu* Bally *et al.* 1986; Barchi *et al.* 1998*a*, *b*, *c*; Mirabella *et al.* 2008).

In the interpreted sections, two other seismic units, referred to as TC (T = Tuscan tectonic unit; C = Carbonates) and REN (Rentella tectonic unit) were traced, whose presence is solely predicted based on the regional stratigraphic framework since they were not encountered by the Pratomagno1 Well.

Seismic unit TC consists of wedge-shaped bodies characterized by transparent reflections, bounded by mid to high-amplitude and low-frequency reflectors, in the western part of SL-1. It is interpreted as carbonates of the Tuscan tectonic unit, i.e. the Mesozoic calcareous substrate of the Scaglia Toscana Fm..

Seismic unit REN is characterized by high-amplitude and low-frequency reflectors and interposed between the base of the allochthonous Tuscan tectonic unit (TMA+TSC) and the top UMA.

The seismic interpretation is furthermore based on the identification of three key seismic marker horizons (Fig. 5):

(1) M1: Top Scaglia Toscana Fm. (Top seismic unit TSC), top of a group of closely spaced, high amplitude, medium-continuity reflectors, with a thickness of 0.2–0.3 s (TWT);

(2) M2: Top Umbria Carbonates (Top UCE), upper reflection of two parallel, high-amplitude, high-continuity reflectors, spaced about 0.2 s (TWT), which marks the position of the Top of Calcareous Scaglia and the Top Marne a Fucoidi Fm., thus tracing the position of the upper part of the Umbria Carbonates;

(3) M3: Top Acoustic Basement (Top UBA), the almost transparent seismic facies of the Umbria Carbonates and Evaporites, is bounded at its base by a group of discontinuous, high-amplitude reflectors, defining the acoustic basement (*sensu* Bally *et al.* 1986; Mirabella *et al.* 2008).

The correlation with the Pratomagno1 well (Fig. 5), showing the superposition of TMA, TSC, UMA, UCE, controls the calibration of the markers M1 and M2 in the seismic profiles SL-a and SL-b. The comparison of the main reflectors in the seismic profiles (SL-1, SL-2, SL-3) and their intersections, correlates the Umbria units UMA, UCE, UBA and the reflectors M2 and M3. The comparison with previous interpretations of adjacent regions (Western Umbria in particular, see e.g. Mirabella *et al.* 2004; 2011) further supports the proposed seismic stratigraphy. For the M1 marker, further control is offered by the correspondence between the reflector and the outcrops of Scaglia Toscana in the study area.

4.c. Seismic interpretation and depth conversion

The three seismic profiles crossing the study area were all interpreted using the 3 marker reflections and the seven seismic units as key building elements. The interpretation of seismic lines SL-2 and SL-3 was mainly used for structural framework interpretation of the study area. The integrated section balancing approach presented in the following focuses on the seismic line SL-1, which crosses the study area transversally and offers a complete strike-perpendicular view into the OTN wedge.

4.c.1. SL-1 profile

At relatively shallow depth, the profile SL-1 (Fig. 6) shows a prominent package of high-amplitude reflectors interpreted as the Scaglia Toscana Fm. (TSC), which regionally corresponds to the basal décollement of the OTN (TMA + TSC), that becomes progressively shallower from the southwest (1.5 s - TWT- at 10 km) to the northeast (0.6 s - TWT- at 24 km). The major splays of the imbricate thrust system splaying out from this basal décollement are particularly evident in the central part of the profile (between 10 and 24 km) whilst, towards the northeast, the seismic reflections, become more chaotic and discontinuous. The geometry of the OTN wedge to the northeast was chiefly reconstructed on the base of surface geology data.

At the western end of the profile, between 0 and 10 km, there are two sigmoidal reflection packages bound by medium to high-amplitude and low-frequency reflectors that pinch-out westward below the TSC. The reflection packages were tentatively associated with the TC, as also proposed in previous interpretations (Barchi *et al.* 2013).

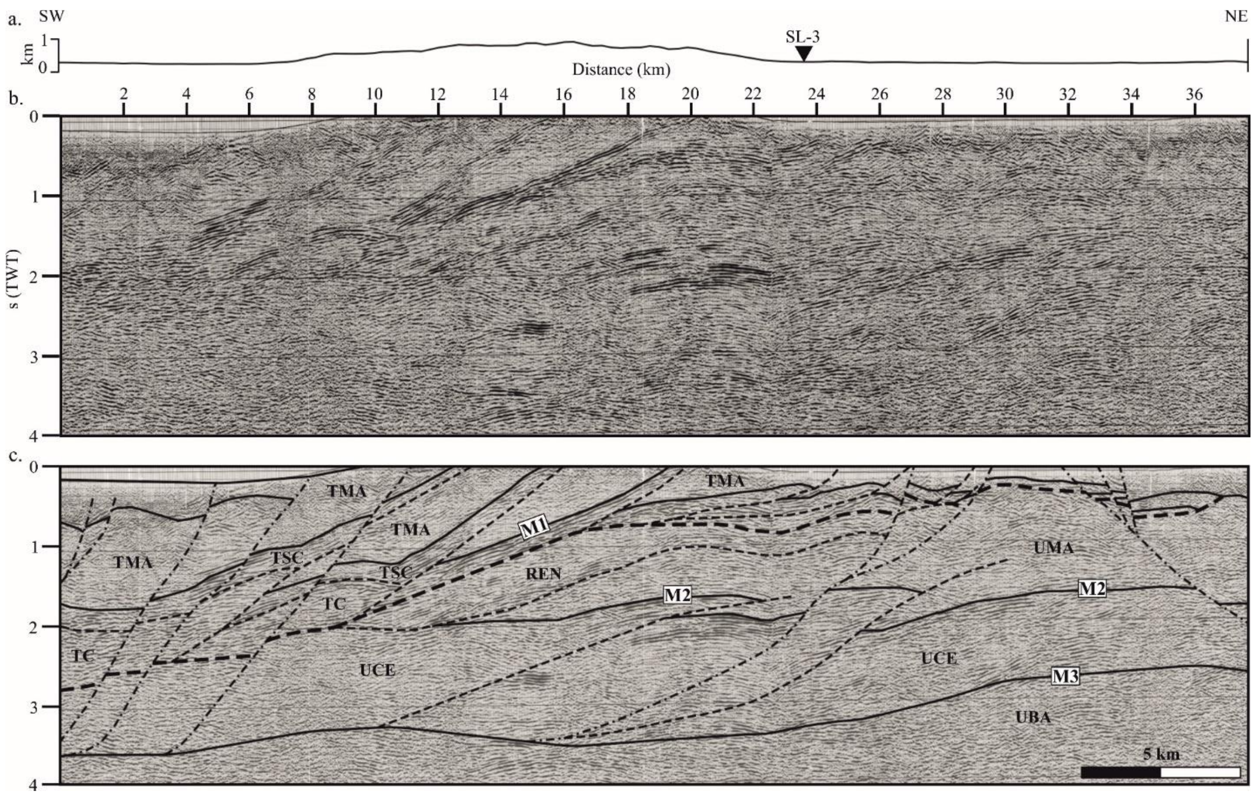

Fig. 6. (a) topography distribution above the SL-1 trace. (b) seismic profile SL-1 in TWT. (c) interpretation showing the main tectonic features. Full lines are lithological contacts, dashed lines are thrust faults, dashed-dotted lines are normal faults.

In the central part of the seismic line, the M2 horizon traces the top of the UCE, forming a long-wavelength anticline structure culminating at 1.7 s (TWT). Local doubling of M2 (e.g. between km 17 and 24) marks the involvement of the UCE in thrusting. In the deepest part of the profile, the underlying acoustic basement (M3) coincides with high-amplitude, low-frequency reflectors, dipping westward between around 2.6 s and 3.8 s (TWT).

In the central part of the profile (between 12 and 18 km), about 0.5 s (TWT) beneath the base of the OTN, a prominent west-dipping reflection is interpreted as the base of the REN, which crops out about 10 km southward of the interpreted section east and southeast of the Trasimeno Lake, interposed between the OTN and the TMA (Fig. 2) (Brozzetti *et al.* 2000; Meneghini *et al.* 2012).

All along the profile, several normal faults were recognized that displace the stacked compressional structures. Both SW-dipping and NE-dipping normal faults, recognized at both edges of the profile, displace the OTN creating accommodation space for the post-orogenic deposits of the Val di Chiana Basin to the west and of the High Tiber Basin to the east (Fig. 2), with a maximum thickness of 0.3 s (TWT).

4.c.2. SL-2 profile

The seismic line SL-2 (Fig. 7), located about 10 km north with respect to SL-1, with a SW-NE orientation, is 12 km long and intersects SL-3 at km 5. Similar to SL-1, SL-2 clearly displays at shallow depth the internal imbrication of the OTN, expressed by a set of high-amplitude reflectors associated to the TSC, showing two major imbrications, detached above a southwest-dipping basal décollement, localized between 0.5 s and 1 s (TWT).At intermediate depth (1.5 to 2.5 s TWT), reflector M2 is folded and displaced by a SW-dipping thrust fault and the related hanging-wall anticline, whilst the footwall is less deformed, showing a regular, gently west-dipping geometry.

In the eastern part of profile SL-2 (progressive 10 km at the surface), both M1 and M2 are displaced by a major SW-dipping normal fault, reaching a depth > 3 s (TWT) at the western end of the profile.

In the southwestern part of seismic line SL-2 (Fig. 7), between km 0 and 7, interposed between TSC and M2, a set of prominent west-dipping reflectors is associated with the REN, in line with the interpretation proposed for SL-1. At greater depth, between 3 s and 3.5 s (TWT), the strong reflections of the M3 appear slightly folded and unaffected by thrusting. Within the UBA Unit, various secondary internal reflectors can be recognized. In the north-eastern part of the profile, the distance between M2 and M3 (0.9 s TWT) is representative of the stratigraphic thickness of the UCE.

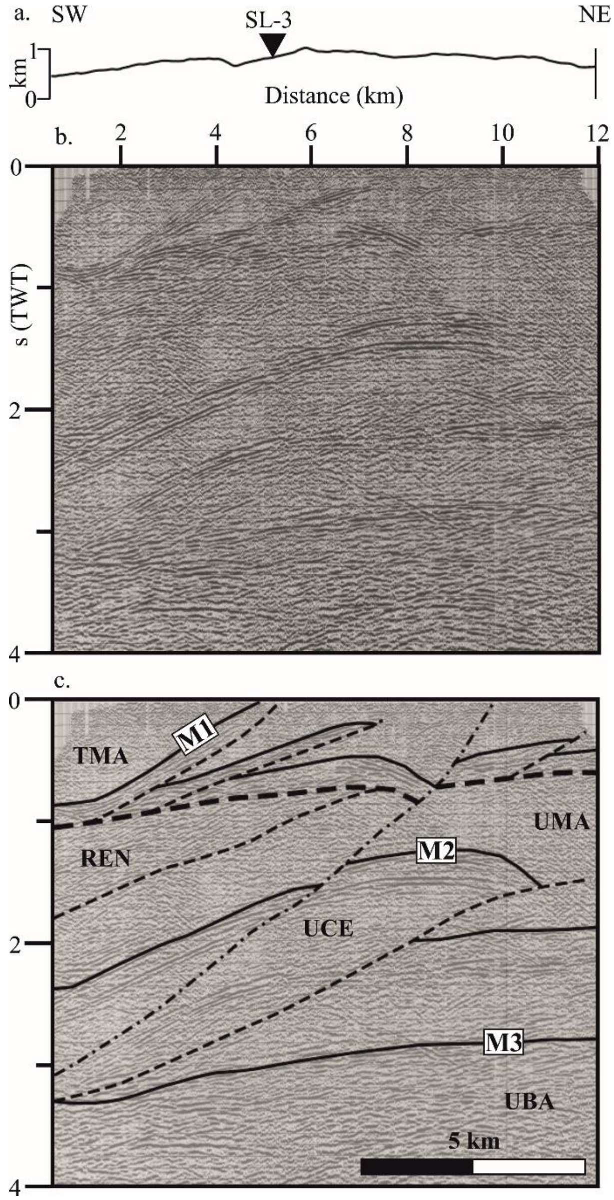

Fig. 7. (a) topography distribution above the SL-2 trace. (b) seismic profile SL-2 in TWT. (c) interpretation showing the main tectonic features. Full lines are lithological contacts, dashed lines are thrust faults, dashed-dotted lines are normal faults.

4.c.3. SL-3 profile

The NW-SE oriented seismic line SL-3 (Fig. 8) crosses longitudinally the main structures of the study area. It is 25 km long and intersects both SL-2 and SL-1 at km 9 and km 13 respectively. The uppermost part of the SL-3 section (down to about 1s) images the OTN, bounded at its base by its basal décollement.

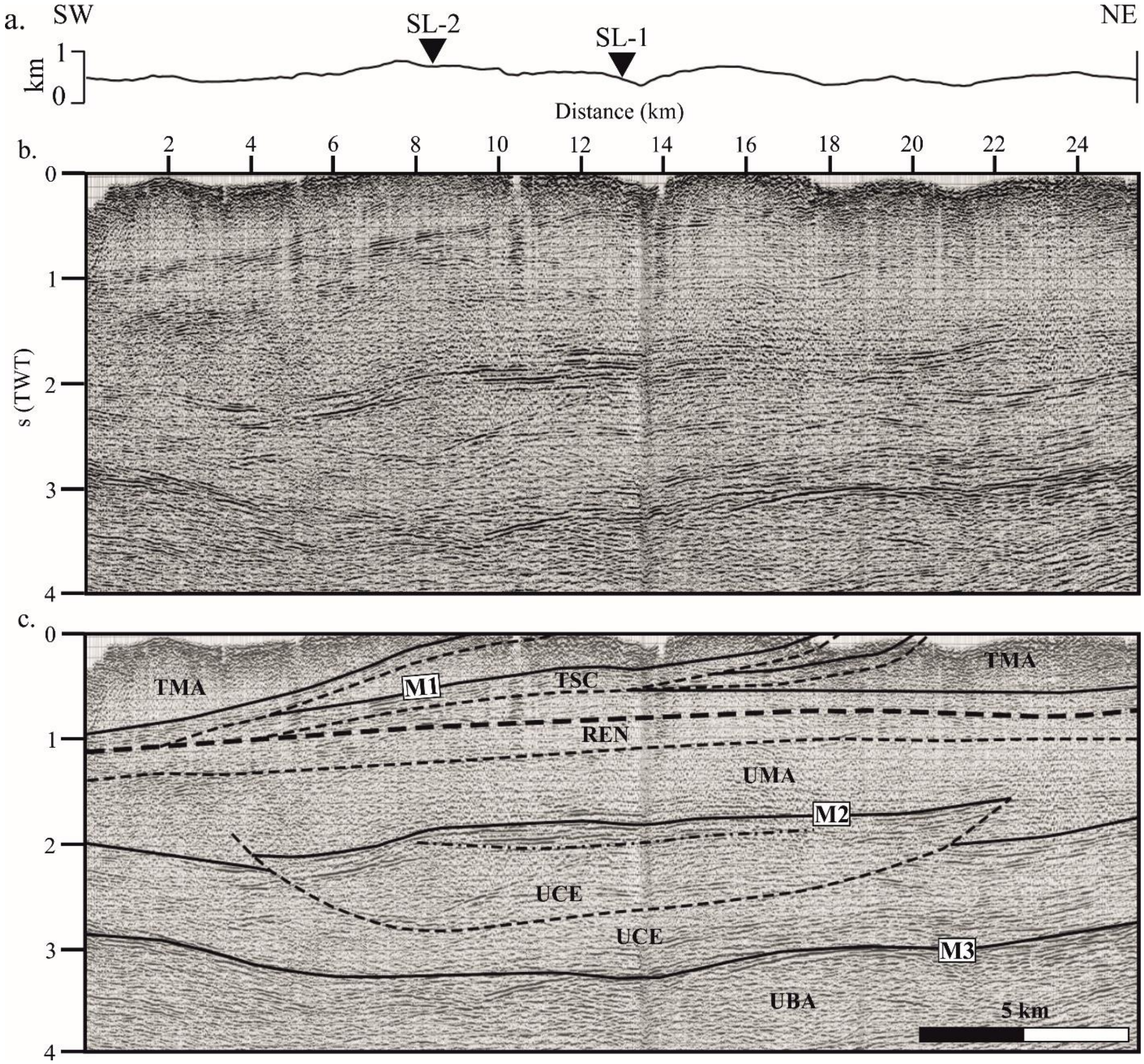

Fig. 8. (a) topography distribution above the SL-3 trace. (b) seismic profile SL-3 in TWT. (c) interpretation showing the main tectonic features. Full lines are lithological contacts, dashed lines are thrust faults, dashed-dotted lines are normal faults.

Three main packages of TSC splay out from the almost flat basal décollement, imaging a set of imbricate thrust faults, with an apparent dip toward the NW. All along the profile, below the basal décollement, the REN is homogeneously distributed with a thickness in the order of 0.3 s (TWT) overlying the UMA.

Between 1.5 s and 1.9 s (TWT), M2 is recognized to be faulted at km 3 and 22 by a single thrust fault, cut along strike, with the transport direction perpendicular to the profile, showing opposite dip in its NW-ward and SE-ward terminations. Because of thrust faulting, the true stratigraphic thickness of the UCE (~ 0.9 s TWT) can be estimated only in the footwall blocks at the opposite sides of the profiles, while in the central part of the profile, the UCE is tectonically thickened (up to 1.4 s TWT). In the proposed interpretation, this thrust does not affect the underlying top basement M3, located between 2.7 s and 3.2 s (TWT).

4.c.4. Depth conversion

A simplified time-to-depth conversion of the three seismic profiles was performed by using interval velocities (see Fig. 5a), derived from previous works (Bally *et al.* 1986; Barchi *et al.* 1998*a*, *b*, *c*; Mirabella *et al.* 2011) that averaged log velocity data recorded in various exploration wells of the region. Coherently with the cited studies, the interval velocities (Vp) within each seismo-stratigraphic unit were assumed to be constant with depth and laterally. Figure 9 shows the interpretation of seismic line SL-1, chosen as a representative to draw a geological cross-section of the study area, integrated with surface geology data.

5. Section integration and timing of deformation

5.a. Surface-subsurface integration

By combining surface data (i.e. geological maps and the geological cross section B, Fig. 4b) and subsurface data converted to depth (SL-1, Figs. 6, 9), we obtained a 33 km long, WSW-ENE trending, integrated geological cross-section that shows the internal geometry of the imbricate thrust system of the OTN tectonic wedge and of the underlying Umbrian siliciclastic turbidites and carbonates, down to the top of the acoustic basement (Fig. 9c).

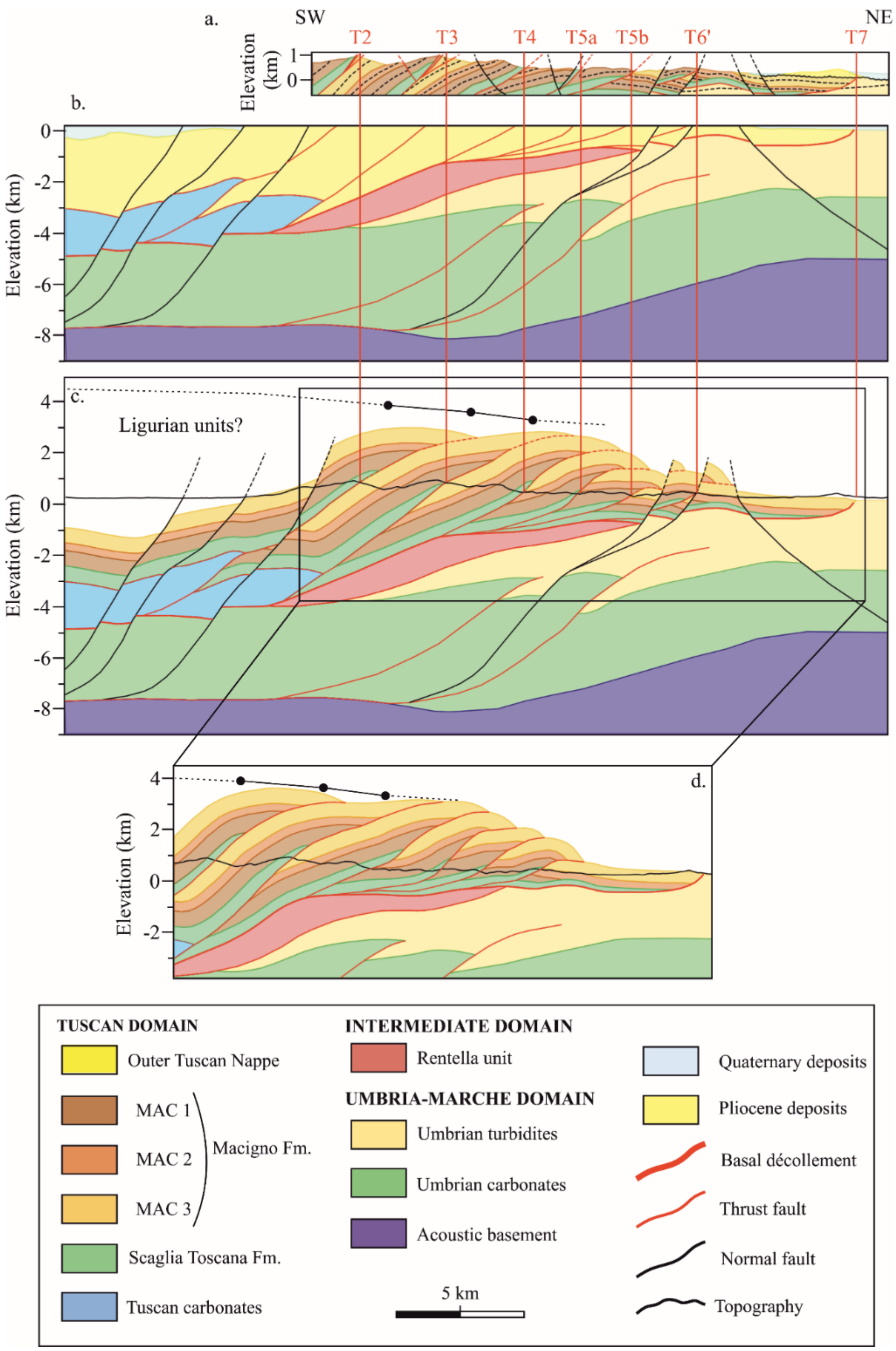

Fig. 9. (a) geological cross section B. (b) interpretation of the SL-1, projected onto the geological cross section B and subsequently converted in depth. (c) final integrated section displaying the reconstructed OTN tectonic wedge geometry. Black dots represent the values of maximum burial depth obtained by Caricchi *et al*. 2015*a*, re-projected onto the integrated section and are fitted by a line which represents the extrapolated maximum thickness of the OTN. (d) zoom on the upper part of the wedge, after the restoration of the extensional faults to demonstrate how the reconstructed wedge fits thermal and burial data by Caricchi *et al*. 2015*a*.

The reflections interpreted as thrust faults on the seismic sections show a good correspondence with the thrust faults exposed at the surface. The seismo-stratigraphic units attributed to the Macigno Fm. and the Scaglia Toscana Fm. are also in agreement with respective surface exposures. In the western and central part of the section, the basal décollement of the OTN wedge, as well as the trajectories at depth of the internal splays, are well constrained by the seismic data. On the contrary, in the eastern part of the section, the seismic image of the basal décollement is unclear, possibly due to a lower thickness of the tectonic wedge and to the effects of younger normal faults which cause complex deformation patterns. For this reason, in the easternmost part, the proposed reconstruction is largely based on the surface geology. The interpretation of the deepest units in the footwall of the OTN wedge, including the Rentella intermediate tectonic unit (REN), the Umbria-Marche turbidites (UMA) and the underlying Umbria-Marche carbonates and evaporites (UCE), down to the Top of the acoustic basement (UBA), is entirely based on seismic data interpretation.

In order to reconstruct the original OTN wedge geometry at the time of its emplacement (i.e. before the main erosional phase and the subsequent extensional tectonics), the integrated section was extended above the topography (Fig. 9c) using the following approach.

The Top Scaglia Toscana Fm. (M1), as constrained by both, surface and subsurface data, was used as the key-horizon to estimate the actual displacement associated to each thrust of the imbricated system. In all interpreted profiles, the footwall cut-off of TSC is well imaged and constrained by the seismic data, as the TSC is marked by a group of prominent reflections. The seismic data also constrain the position of the hanging wall cut-off for the easternmost thrusts, where the TSC is not exposed at the surface. For the western thrusts, the position of the hanging wall cut-off is determined based on surface geology data.

Above the Top Scaglia Toscana Fm. (M1), the thickness, geometry, and elevation of the different members of the Macigno Fm. were also derived from the surface geological data (synthesized along the surface geological cross sections, see Fig. 4b). The Macigno Fm. was extended above the topography maintaining a conservative interpretation of the thickness of the OTN wedge, i.e. using the same stratigraphic thickness estimated in the field.

5.b. Timing of deformation

The tectonic history of the study area can be subdivided by structural restoration into six key time intervals. In the first interval (Fig. 10a), Rupelian to early Aquitanian in age, initial foredeep formation occurred in response to the emplacement and imbrication of the Ligurian tectonic units. During this interval, the deposition of the Macigno Fm. (Chattian–Aquitanian) was coeval with the deposition of the pelagic marls of the Rentella intermediate domain (Rupelian–Aquitanian) in the easternmost foreland ramp (Meneghini *et al.* 2012). In the second interval (Fig. 10b), late Aquitanian to early Burdigalian in age, the OTN wedge internal imbrication drove the onset and evolution of the foredeep basin in which the siliciclastic turbidites of the upper Rentella intermediate domain were deposited. In the third interval (Fig. 10c), middle to late Burdigalian in age, the eastward migration and emplacement of the OTN wedge and the deformation of the Rentella tectonic unit occurred during the deposition of the inner Marnoso-Arenacea Fm.. In the fourth interval (Fig. 10d), early Serravallian in age, the deep-seated deformation of the Umbrian carbonates and evaporites unit caused an eastward shift of the Umbria foredeep depocenter (Brozzetti, 2007). The thrust faults deforming the Umbria carbonates and evaporites detached at the top basement, and produced further shortening by folding and passively transporting the OTN wedge eastward. Subsequently, in late Serravallian time (Fig. 10e), progressive uplift and erosion of the OTN wedge occurred, as suggested by the lack of sediments of this age in the study area and by the occurrence of olistostromes consisting of deformed Ligurian units further to the east (Ricci Lucchi & Pialli, 1973).

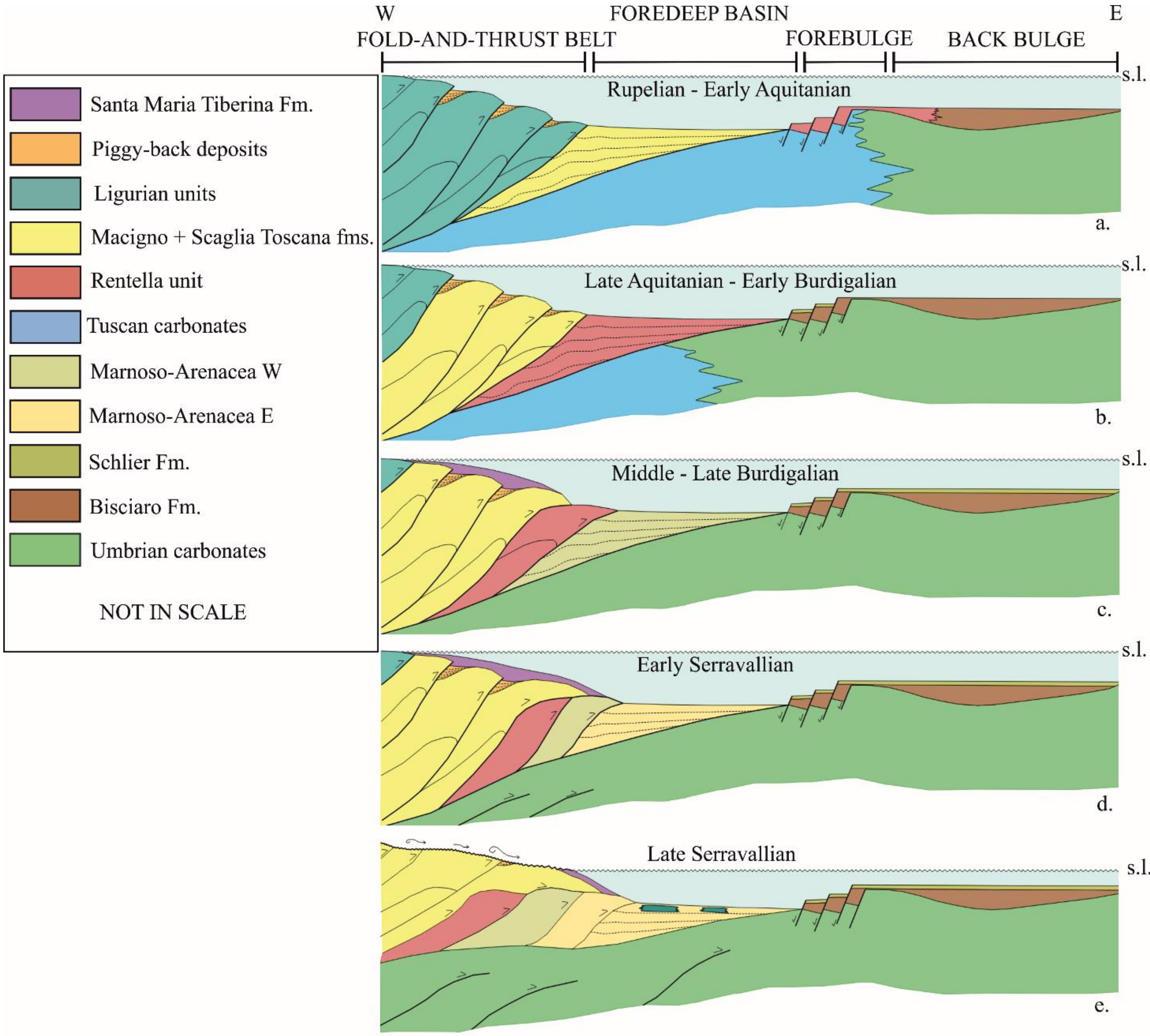

Fig. 10. Model proposed for the evolution of the study area displaying the tectonic units in their structural position. (a) inner belt made up by the Ligurian units and end of the Macigno Fm. deposition. (b) Tuscan units involved in the tectonic wedge and end of deposition of the Rentella tectonic unit in foredeep basin. (c) deposition of the Monte Santa Maria Tiberina Fm. on the top of the tectonic wedge, end of active deformation of the OTN and deposition of the inner Marnoso-Arenacea Fm. (d) eastward migration of the wedge, deep deformation of the Umbrian carbonates and evaporites and deposition of the outer Marnoso-Arenacea Fm. (e) main erosional phase characterized by olistostromes of eroded Ligurian units within the Marnoso-Arenacea Fm.

During the Tortonian, the compressional front of the FTB migrated further eastward: the Umbria foredeep reduced to a narrow trough (M. Vicino piggy-back basin; e.g. Centamore *et al.* 1977; Lena *et al.* 2014). In the Pliocene and Quaternary, extensional tectonics finally disrupted the compressional belt and drove the evolution of the Val Di Chiana and High Tiber basins (e.g. Barchi, 2010; Gasperini *et al.* 2010).

6. Discussion

Many geological concepts for the early contractional deepwater evolution of FTBs are derived from marine seismic-reflection imaging and interpretation of modern deepwater systems (e.g. Krueger & Gilbert, 2009; Morley *et al*. 2011 and references therein). In contrast to fossil FTBs, modern DWFTBs have the advantage of being not yet affected by a later stage orogenic structural overprint, and they are covered in many cases by an extensive, high-quality, potentially 3D seismic database (locally supported by well data). Limits of dominantly or exclusively seismic-based DWFTB studies include i) problems in the seismic-reflection display of steep or overturned bedding, ii) the loss of seismic energy with depth and thus a downward decrease in seismic resolution and the signal-to-noise ratio, and iii) general resolution limits that hamper the analysis of sub-seismic deformation (e.g. minor folds and thrusts at mesoscopic scale; layer-parallel shortening due to tectonic compaction; sedimentary compaction; sub-grain deformation), which can account for additional (up to 50%) shortening in contractional systems (e.g. Cooper e*t al*. 1983; Morley, 1986; Mitra, 1994; Koyi, 1995; McNaught & Mitra, 1996; Koyi *et al*. 2003; Ghisetti *et al*. 2016). In contrast, combined surface-subsurface studies of fossil onshore FTBs can integrate field mapping results and structural outcrop analysis, which enables to better constrain i) fold and anticline geometries at any scale, ii) true shortening accommodated by thrusting and folding at any scale, iii) shortening distribution and iv) physical properties of both thrusted stratigraphy and individual tectonic structures. The inherent disadvantage of a younger structural overprint within fossil, exposed FTBs can be overcome by consequent tectonic reconstruction.

6.a. Geometric reconstruction of the OTN

In the integrated section of Figure 9, the basal thrust of the OTN wedge has a flat-ramp-flat geometry and becomes progressively shallower from W to E. The westernmost flat part of the décollement is located below the carbonates of the Tuscan Domain, and its depth varies, from west to east, between 4.6 km and 3.2 km. The stratigraphy of the Tuscan Domain varies accordingly in thickness, from 4 km in the west to ~ 1km in the east. The décollement is warped above the Rentella tectonic unit, and becomes flat in the easternmost part; here, the wedge is detached above the Scaglia Toscana Fm. and the décollement shallows toward the east from a depth of around 3.2 km to around 1 km. Consequently, the OTN wedge is up to 5 km thick and tapers progressively eastward.

The OTN wedge geometry and thickness, as reconstructed in the geological cross-section of Figure 9, has been compared with recent thermal burial data, produced by Caricchi *et al.* (2015*a*), by using a combination of different techniques (XRD, vitrinite reflectance, clay minerals crystallinity degrees, carbon and oxygen stable isotopes analyses). These authors estimate a maximum burial depth decreasing eastward from 3.7 km for the most internal thrust to 2.3 km, values which are slightly higher than those reconstructed in this study (Figs 9c, d).

In agreement with Caricchi *et al.* (2015*a*), we can hypothesize that a sheet of Ligurian tectonic units originally covered the OTN, tapering towards the east. At present, however, in the area crossed by the geological section, the Ligurian tectonic units are exposed only in limited outcrops, scattered on the southwestern side of the Lake Trasimeno (Fig. 2; Barchi *et al.* 2010). Much larger outcrops of Ligurian tectonic units are exposed north of the High Tiber Basin (Fig. 2), where emplacement is thought to be due to large-scale gravity sliding in the late stages of the Northern Apennines history (e.g. De Feyter, 1991). This distribution can be explained either by intrinsic uncertainties in the thermal burial estimations or by the occurrence of syn-tectonic piggy-back deposits, once placed upon the Macigno wedge which are today eroded.

After its emplacement, the OTN tectonic wedge underwent uplift and erosion, possibly related to both later phases of the orogenic process and to subsequent post-orogenic extension (e.g. Jolivet *et al.* 1998; D'Agostino *et al.* 2001). By comparing the geometry of the integrated section with the present-day topography (Fig. 9c), and coherently with the thermal burial data, we can conclude that up to 3 km of rocks have been eroded, mostly consisting of turbidites of the Tuscan Domain and possibly an outermost sheet of the Ligurian tectonic unit.

In the attempt to establish the timing of this uplift/erosional stage, it has to be kept in mind that: i) uplift certainly started after the final OTN emplacement (late Burdigalian); ii) no other sediments of Miocene age are exposed in the study area covering the eroded Macigno turbidites; iii) some sediment stemmed from syn-sedimentary reworking of strata outcropping in the study area, which can be e.g. recognized in turbiditic successions exposed between the High Tiber Basin and the main mountain ridge of the Northern Apennines (Umbria pre-Apennines, *sensu* Bally *et al.* 1986); transversal supply of arcosic or hybrid arenite, as well as olistostromes of Ligurian-Epiligurian provenance, are frequent within the Langhian–Serravallian Marnoso-Arenacea Fm., whilst the Tortonian and Messinian piggy-back basins of the region are constantly filled by turbidites fed from the west (e.g. Alvarez, 1999); and iv) in the Val di Chiana Basin (e.g. Aruta *et al*. 2004), as well as in the Trasimeno Lake area (e.g. Gasperini *et al*. 2010), Macigno Fm. sandstones are unconformably covered by early Pliocene marine sediments, whose deposition mark the end of the main uplift/erosion phase. After this time, the region experienced only limited uplift, as indicated by the present-day elevation of both early Pliocene and early Pleistocene paleo-coasts not higher than 400 m a.s.l. (Ambrosetti *et al*. 1978).

The above observations indicate that most of the uplift and erosion of the OTN wedge occurred in late Burdigalian to Messinian time. It is particularly worth to note that a major erosional phase of the emerged lands of the Paleo-Apennines was associated with the Messinian salinity crisis that culminated ~5.7 Ma (Hsü *et al.* 1972; Ryan & Cita, 1978) and led to a dramatic drop of the river base level (e.g. Scarselli *et al.* 2007).

Considering a period of 10 Ma between the late Burdigalian and the late Messinian as well as a thickness of the removed material of around 3 km, the estimated long-term, averaged erosion rate should be about 0.3 mm/yr. Bartolini *et al.* (2003) suggested a long-term average exhumation rate for the Northern Apennines of about 0.7 mm/yr since 11 Ma. At shorter time-scales, Picotti & Pazzaglia (2008) and Wegmann & Pazzaglia (2009) provided uplift rates of about 0.2 and 0.5 mm/yr between 190 and 140 ka. Using speleological data, Mariani *et al*. (2007) estimated an uplift rate of the Apennine ridge of about 0.6 mm/yr during the Holocene. Thomson *et al.* (2010), based on an extensive regional apatite (U-Th)/He thermo-chronometric database augmented by pre-existing apatite fission-track (AFT) data, measured an exhumation rate for the extending internal, retro-flank of the Apennine orogen of ~ 0.3–0.5 mm/yr over a period of ~ 3–5 Ma. These values are in the order of present-day erosion rates (0.2–0.6 mm/yr) determined by means of ^{10}Be concentrations on modern and middle Pleistocene sediments in the Romagna Apennines, NW of the study area (Cyr & Granger, 2008).

6.b. Kinematics

During the 2D restoration process (Fig. 11) we measured the shortening of the OTN wedge focusing on two distinct processes: the internal imbrication of the allochthonous Tuscan tectonic units (i.e., Macigno and Scaglia Toscana fms.) and their eastward emplacement over the Rentella Intermediate Domain and the Umbria-Marche Domain above the basal décollement.

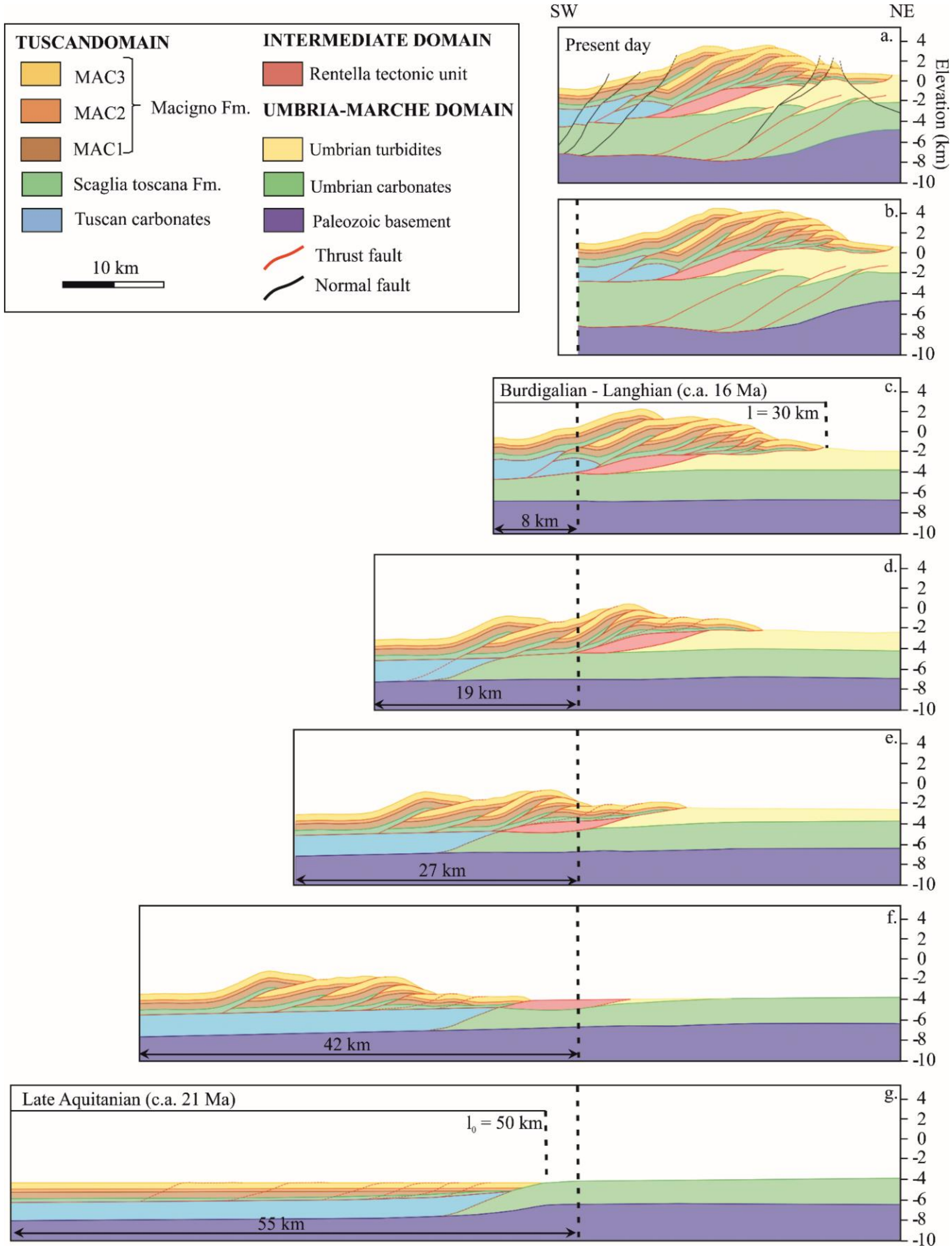

Fig. 11. 2D sequential restoration. (a) Present-day. (b) Normal faults restoration. (c) Restoration of the deep thrusting involving UCE. (d) Backward translation of the OTN, restoration of thrusting affecting TC and the outermost thrust faults. (e) Restoration of REN; (f) Final backward translation of the OTN. (g) Restoration and unfolding of the internal imbrication within the OTN.

In the geometric reconstruction, about 20 km (40%) of shortening was achieved by internal imbrication of the wedge, measured along the Scaglia Toscana Fm., taking into account a final length (l) of 30 km and an initial length (l_0) of 50 km (Figs. 11c-g). Across the wedge, shortening associated with the single thrust units decreases towards the frontal thrust fault (i.e. eastward) from values of about 7 km in the western part of the wedge to values of around 1 km in the eastern part (Table 2). Note that the basal décollement deepens westward so that the lower carbonate unit of the Tuscan Domain is involved in the westernmost thrusts (e.g., T2 and T3).

SHORTENING (km)								
Internal imbrication						Active transport		Passive transport
T2	T3	T4	T5a	T5b	T6'	BD	REN	UCE
7	5.3	3	1.9	1.5	1.3	23	14	3
Internal shortening						Total transport		
20 (40%)						40		
Total Bulk Shortening								
60								

Table 2. Components of the total bulk shortening measured along the integrated section.

Simultaneously, or soon after its internal imbrication (Fig. 11f), the OTN wedge was transported eastward a further 23 km along its basal décollement, overthrusting the turbidites of the Rentella intermediate tectonic unit (REN) (Figs. 11e) and the innermost Umbrian turbidites (Fig. 11d). Summing up the two contributes, the total shortening of the OTN wedge is about 43 km.

After the final emplacement of the OTN wedge, the tectonic units in its footwall experienced further shortening: the REN was transported over the Umbrian turbidites (Marnoso-Arenacea Fm.)

for about 14 km, and the lowermost Umbrian units (carbonates and evaporites) were in turn folded and faulted, with a shortening of ~ 3 km (Fig. 11c). Considering this further deformation, the measured total bulk shortening of the integrated geological section is ~ 60 km.

The Monte Santa Maria Tiberina Fm. provides an important kinematic constraint because it is recognized to seals the OTN leading edge (see Fig. 4b), postdating the Marne di Vicchio Fm. (Lucchetti *et al.* 2002; Brozzetti, 2007). According to this reconstruction, the internal imbrication of the OTN wedge and its emplacement over the Umbrian turbidites happened between two major sedimentary events, i.e. the end of the deposition of the Macigno Fm. (late Aquitanian) and the start of the deposition of the Monte Santa Maria Tiberina Fm. (late Burdigalian). The emplacement of the OTN is therefore bracketed in the late Aquitanian–late Burdigalian time interval, corresponding to a duration of about 5 Ma. This timing is in agreement with the tectonic evolution proposed by Caricchi *et al.* (2014), mainly based on paleomagnetic data. Considering the total amount of shortening (20 + 23 km = 43 km) and the corresponding timing of deformation (5 Ma), the estimated average deformation rate was ca. 8.6 mm/yr. However, it is worth to note that considering the internal imbrication only, the resulting shortening rate is in the order of 4 mm/yr.

The emplacement of the Rentella intermediate tectonic unit over the turbidites of the Umbria-Marche Domain and the internal deformation of carbonates of the Umbria-Marche Domain both post-date the emplacement of the OTN wedge. In particular, the deformation of the deep-seated carbonates of the Umbria-Marche Domain could be coeval to that of the analogous anticline, responsible for folding the OTN external thrust in the Mt. S. Maria Tiberina area (Brozzetti, 2007), which occurred in middle–mate Serravallian, synchronous with the deposition of the Marnoso-Arenacea Fm., east of the Tiber Basin (Fig. 2).

A similar structural setting can be observed in the Agri Valley sector of the Southern Apennines, where allochthonous units of Triassic to Palaeogene shallow-water carbonate platform and pelagic basin successions deposited in the Apenninic Platform and Lagonegro Basin, respectively, are completely detached from their original substratum and transported towards the east onto the foreland carbonates of the Apulian Platform, accommodating around 35% of internal shortening (Mazzoli *et al*. 2001).

6.c. Mechanics

In order to estimate the possible values of fault (F) and wedge (W) strength of the OTN, the values of critical-wedge taper were plotted in an F/W diagram firstly proposed by Suppe (2007) and subsequently modified by King & Morley (2017) who rearranged the original critical-taper equations (Davis *et al.* 1983; Dahlen, 1990). The F vs. W diagram (Fig. 12) constrains all possible values of the two parameters F and W, solely based on the wedge-taper angle measurement, excluding the values of pore pressure and the coefficient of friction. F and W represent the basal detachment strength, and the overburden strength (the crust surrounding the faults), respectively.

Along the regional cross-section (Fig. 9), the measured value of the wedge-taper has an average value of about 8°, with some uncertainties due to its not-planar geometry. In the present-day setting, the dip of the basal décollement (β) is about 2°, whilst the top of the wedge slope (α) is about 6°. However, the geometry of the OTN wedge could have been modified during uplift, or locally affected/tilted by recent extensional tectonics. Mariotti & Doglioni (2000) measured the dip angle of the regional monocline all along the present-day frontal part of the Apennines from published seismic data, unpublished industrial seismic data and regional geological balanced cross-sections, suggesting an average β angle of 8° and an almost flat (or even locally hinterland-sloping) top surface. Following these uncertainties, plotting the OTN case study in the diagram of

King & Morley (2017), all the possible values of α and β, ranging from 0° to 8° were considered (Fig. 12).

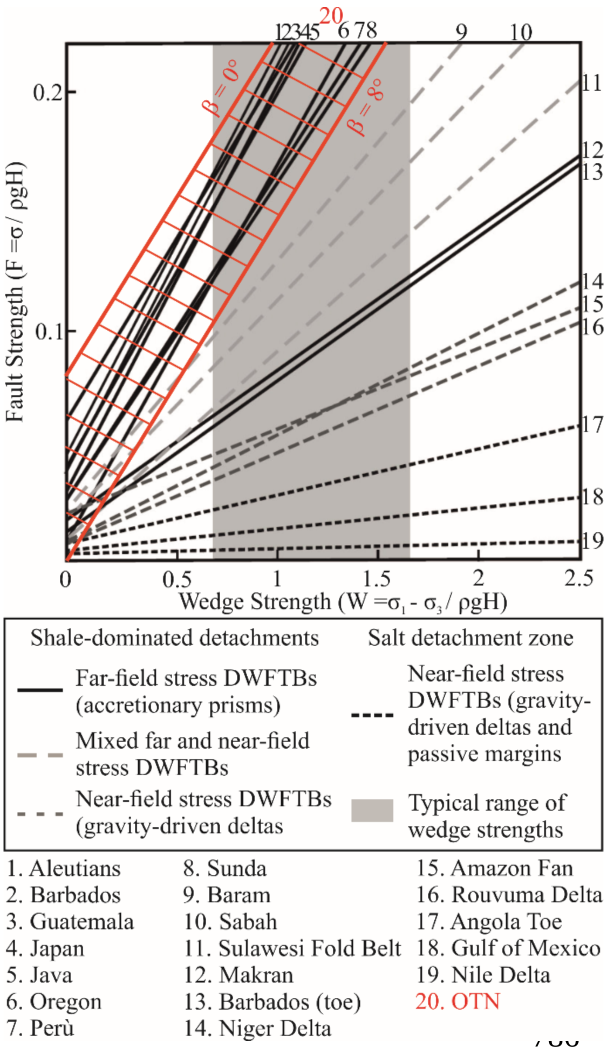

Fig. 12. Plotted values of the OTN critical wedge. The range of values of α and β between 0° and 8°, considering a critical-taper angle of 8°, falls in the Far-field stress DWFTBs field of the Plot of Fault strength (F) vs. Wedge strength (W). Modified after King and Morley, 2017.

Therefore, we obtained a range of W and F values for the OTN, which, as expected, fall in the plot field for far-field-stress DWFTBs. The same range of values includes several examples of accretionary prisms; this suggests that early-stage foreland FTBs (i.e. the OTN) and accretionary prisms have similar mechanical characteristics concerning e.g. lithological composition or overpressure at the detachment level. The result of the F/W plot can be compared e.g. with the W Nankai, Java, Costa Rica accretionary prisms (see Tesei *et al*. 2015 and King & Morley, 2017 for reviews), or with foreland FTBs including the Rocky Mountains of Southern Canada and the

Mexican FTB of Central Mexico, which show wedge taper angles of 6°–8.3° and 5°–6.3°, respectively (Fitz-Diaz *et al*. 2011).

7. Conclusions

This study provides new insights about the geometry and kinematics of the OTN wedge, and also on its mechanical behaviour. The seismic interpretation of the OTN shows that i) its structural style is characterized by a series of thrust faults splaying out from a basal décollement identified as the Scaglia Toscana Fm.; ii) its basal décollement shallows eastward, from a depth of around 3.2 km to less than 1 km; iii) it was transported over the outermost Rentella and Umbria domains for a distance of more than 20 km; iv) the Rentella tectonic unit was later superposed onto the autochthonous Umbria-Marche domain, which experienced later folding and thrusting.

The construction of an integrated surface-subsurface section allowed to reconstruct the original OTN wedge geometry, showing that: i) the spacing between the imbricated thrust faults, the width, the thickness and the displacement of the tectonic units, as well as the dip angle of each thrust fault tend to decrease eastwards, which are characteristics of in-sequence deformation; ii) the tectonic wedge was up to 5 km thick in its central-western part and tapers progressively eastward thinning down to around 1 km; iii) the reconstructed wedge-taper angle was around 8°.

Structural restoration showed that the OTN wedge experienced a total shortening of 43 km, comprising 20 km (40%) of internal imbrication and 23 km of eastward translation above its basal décollement. The shortening, accommodated by each thrust fault, decreases towards the frontal thrust. The emplacement of the OTN is constrained to the late Aquitanian–late Burdigalian time interval, and the calculated average shortening rate is ~ 8.6 mm/yr. However, taking in account the internal imbrication only, the calculated average shortening rate is in the order of 4 mm/yr, a value comparable with modern cases of early collisional FTBs (e.g. NW Borneo FTB; Carboni *et* *al.* 2019). In this contest it is important to keep in mind that in modern DWFTBs the overall tectonic transport along the basal décollement is often difficult to estimate, producing a likely underestimation of the total bulk shortening of the wedge.

The deeper units at the footwall of the OTN wedge were deformed in the Langhian to Serravallian, with a further shortening of about 17 km, resulting from 14 km eastward translation of the Rentella tectonic unit and 3 km of internal folding and thrusting within the Umbrian carbonates and evaporites.

If interpreted on the basis of the classification of modern DWFTBs (Morley *et al.* 2011), the OTN is in class 2bi (deepwater contractional wedges formed in response to far-field lithospheric stresses). This interpretation is in line with previous studies of the sedimentary facies and ichnofacies of the OTN turbidites (e.g. Delle Rose *et al.* 1994; Mutti *et al.* 1999; Monaco & Trecci, 2014) that indicate that OTN was emplaced in deepwater environment. The restoration results of this study furthermore show high values of internal shortening (40%), an along-dip shortening distribution decreasing towards the frontal thrust (an opposite trend respect to gravity-driven DWFTBs, see Cruciani *et al.* 2017), and a high critical wedge-taper ($\alpha + \beta = 8°$) supporting the interpretation of the OTN as a paradigmatic fossil field analogue for modern DWFTBs driven by lithospheric stresses.

Acknowledgments. We thank the two anonymous reviewers, for their constructive suggestions and comments, which improved the manuscript. We are grateful to ENI for allowing the use and partial reproduction of the seismic data this paper is based on. We thank Gianluca Cornamusini and Paolo Conti for the useful discussion about the timing of emplacement of the OTN. Alba Brobia Ansoleaga is kindly acknowledged for her support with the seismic database. We thank Midland Valley for granting the use of the MOVE software under an academic license. The geological and structural maps were drawn with QGIS software by using the DEM90 from Earth Env. and the bathymetry from NOAA. This research received no specific grant from any funding agency, commercial or not-for-profit sectors.

Declaration of Interest. None

References

ABBATE, E. & BRUNI, P. 1987. Modino-Cervarola o Modino e Cervarola? Torbiditi oligo-mioceniche ed evoluzione del margine Nord-appenninico. *Mem. Soc. Geol. It.* **39**, 19–33.

ALLEN A. P. & ALLEN, J. R. 2005. *Basin Analysis*. Blackwell Science Ltd., second edition, 549 pp.

ALLEN, P. A., CRAMPTON, S. L., AND SINCLAIR, H. D. 1991. The inception and early evolution of the North Alpine Foreland Basin, Switzerland. Basin Research **3**, 143–163.

ALLEN, P. A., BURGESS, P. M., GALEWSKY J. & SINCLAIR, H. D. 2001. Flexural-eustatic numerical model for drowning of the Eocene perialpine carbonate ramp and implications for Alpine geodynamics. *Bulletin Geological Society America* **113**, 1052–1066.

ALVAREZ, W. 1999. Drainage on evolving fold-thrust belts: a study of transverse canyons in the Apennines. *Basin Res.* **11**, 267–284.

AMBROSETTI, P., CARBONI, M. G., CONTI, M. A., *et al.* 1978. Evoluzione paleogeografica e tettonica nei bacini tosco-umbro-laziali nel Pliocene e nel Pleistocene Inferiore. *Mem. Soc. Geol. It.* **19**, 573–580.

ANELLI, L., GORZA, M., PIERI M. & RIVA, M. 1994. Subsurface well data in the Northern Apennines (Italy). *Mem. Soc. Geol. It.* **48**, 461–471.

ARUTA, G., & PANDELI, E. 1995. Lithostratigraphy of the M. Carvarola-M. Falterona Fm. between Arezzo and Trasimeno Lake (Tuscan-Umbria, Northern Apennines, Italy). *Giornale di geologia* **57**(1-2), 131–157.

ARUTA, G., BORGIA, A., BRUNI, P., CECCHI, G., CIPRIANI, N. & TREDICI, Y. 2004. Pliocene and Pleistocene unconformity bounded stratigraphic units (UBSU) in Val di Chiana. In *The "Regione Toscana project of geological mapping* (eds D. Morini & P. Bruni), pp. 133–136. Regione Toscana, Firenze.

BALDACCI, F., ELTER, P., GIANINI, E., GIGLIA, G., LAZZAROTTO, A., NARDI, R. & TONGIORGI, M. 1967. Nuove osservazioni sul problema della Falda Toscana e sull'interpretazione dei flysch arenacei tipo "Macigno" dell'Appennino Settentrionale. *Mem. Soc. Geol. It.* **6**(2), 213–244.

BALLY, A., BURBI, L., COOPER, C. & GHELARDONI, R. 1986. Balanced sections and seismic reflection profiles across the Central Apennines. *Mem. Soc. Geol. It.* **35**, 257–310.

BARCHI, M. R. 2010. The Neogene-Quaternary evolution of the Northern Apennines: crustal structure, style of deformation and seismicity. *Journal of the Virtual Explorer* **36**(10).

BARCHI, M. R., DE FEYTER, A., MAGNANI, M., MINELLI, G., & PIALLI, G. 1998*a*. The Structural Style of the Umbria-Marche fold and thrust belt. *Mem. Soc. Geol. It*. **52**, 557–578.

BARCHI, M. R., MINELLI, G. & PIALLI, G. 1998*b*. The CROP 03 Profile: a synthesis of results on deep structures of the Northern Apennines. *Mem. Soc. Geol. It.* **52**, 383–400.

BARCHI, M. R., DE FEYTER, A., MAGNANI, M., MINELLI, G., PIALLI, G. & SOTERA, M. 1998*c*. Extensional tectonics in the Northern Apennines (Italy): evidence from the CROP 03 deep seismic reflection line. *Mem. Soc. Geol. It.* **52**, 527–538.

BARCHI, M. R., LANDUZZI, A., MINELLI, G. & PIALLI, G. 2001. Outer Northern Apennines. In *Anatomy of an orogen: The Apennines and adjacent Mediterranean Basins* (eds G. B. Vai & I. P. Martini), pp. 215–253. Kluwer Academy Publishers.

BARCHI, M. R., MARRONI, M., BARSELLA, M., BIZZARI, R., BOTTI, F., MENEGHINI, F., PANDOLFI, L., PASSERI, L., PAZZAGLIA, F., ARGENTI, P., BALDANZA, A., CHECCONI, A., CIARAPICA, G., PALANDRI, S., VENTURI, F., BARSELLA, M., BOTTI, F., BOSCHERINI, A., CENCI, M., FELICIONI, G., MENCARONI, B., MOTTI, A., NATALE, G., NATALI, N., PONZIANI, F., SORRENTINO, A., SIMONE, G., BELLUCCI, L.G., BORTOLUZZI, G., GASPERINI, L., PAUSELLI, C. 2010. Carta geologica d'Italia: Foglio 310, Passignano sul Trasimeno scale 1:50.000. *Istituto Superiore per la Protezione e la Ricerca Ambientale,* Rome. http:// www.isprambiente.gov.it /Media.

BARCHI, M. R., CARDELLINI, C., CHECCUCCI, R., FRONDINI, F., FULIGNATI, P., PAUSELLI, C., PAZZAGLIA, F., SBRANA, A., VITERBO, A. 2013. Integrated Multidisciplinary Approach for the Study of the Geothermal Potential of Umbria (Central Italy). *European Geothermal Congress* 2013, Pisa, Italy, 3-7 June.

BARSELLA, M., BOSCHERINI, A., BOTTI, F., MENEGHINI, F., MOTTI, A., PALANDRI, L., MARRONI, M., PANDOLFI, S. 2009. Oligocene-Miocene foredeep deposits in the Lake Trasimeno area (Central Italy): insights into the evolution of the Northern Apennines. *Ital. J. Geosci. (Boll. Soc. Geol. It.)* **128**(2), 341–352.

BARTOLINI, C., D'AGOSTINO, N. & DRAMIS, F. 2003. Topography, exhumation, and drainage network evolution of the Apennines. *Episodes* **26**(3), 212–216.

BENNETT, R. A., SERPELLONI, E., HREINSDÓTTIR, S., BRANDON, M. T., BUBLE, G., BASIC, T., CASALE, G., CAVALIERE, A., ANZIDEI, M., MARJONOVIC, M., MINELLI, G., MOLLI, G. & MONTANARI, A. 2012. Syn-convergent extension observed using the RETREAT GPS network, northern Apennines, Italy. *Journal of Geophysical Research* **117**, B04408.

BOCCALETTI, M., CORTI, G., MARTELLI, L. 2010. Recent and active tectonics of the external zone of the Northern Apennines (Italy). *Int. J. Earth. Sci. (Geol. Rundsch.)* **100**(6), 1331–1348.

BOYER, S., & ELLIOTT, D. 1982. Thrust Systems. *The American Association of Petroleum Geologists Bullettin* **66**(9), 1196–1230.

BROGI, A., CAPEZZUOLI, E., LIOTTA, D., & MECCHERI, M. 2015. The Tuscan Nappe structures in the Monte Amiata geothermal area (central Italy): a review. *Ital. J. Geosci.* **134**(2), 219–236.

BROZZETTI, F. 2007. The Umbria Preapennines in the Monte Santa Maria Tiberina area: a new geological map with stratigraphic and structural notes. *Boll. Soc. Geol. It.* **126**(3), 511–529.

BROZZETTI, F., LUCCHETTI, P. & PIALLI, G. 2000. La successione del Monte Rentella (Umbria Occidentale): biostratigrafia a nannofossili calcari ed ipotesi per un inquadramento tettonico regionale. *Boll. Soc. Geol. It.* **119**, 407–382.

BROZZETTI, F., BONCIO, P., & PIALLI, G. 2002. Early-Middle Miocene evolution of the Tuscan Nappe-Western Umbria Foredeep system: Insights from stratigraphy and structural analysis. *Boll. Soc. Geol. It., Special Volume* **1**, 319–331.

CARBONI, F., BACK, S. & BARCHI, M. R. 2019. Application of the ADS method to predict a "hidden" basal detachment: NW Borneo fold-and-thrust belt. *Journal of Structural Geology* **118**, 210–223.

CARICCHI, C., CIFELLI, F., SAGNOTTI, L., SANI, F., SPERANZA, F. & MATTEI, M. 2014. Paleomagnetic evidence for a post-Eocene 90° CCW rotation of internal Apennine units: A linkage with Corsica-Sardinia rotation?, *Tectonics* **33**, 374–392.

CARICCHI, C., ALDEGA, L., & CORRADO, S. 2015*a*. Reconstruction of maximum burial along the Northern Apennines thrust wedge (Italy) by indicators of thermal exposure and modeling. *Geological Society of America Bulletin* **127**(3/4), 388–438.

CARICCHI, C., ALDEGA, L., BARCHI, M. R., CORRADO S., GRIGO D., MIRABELLA, F. & ZATTIN, M. 2015*b.* Exhumation patterns along shallow low-angle normal faults: An example from the Altotiberina active fault system (Northern Apennines, Italy). *Terra Nova* **27**(4), 312–321.

CARMIGNANI, L., DECANDIA, F.A., DISPERATI, L., FANTOZZI, P.L., KLIGFIELD, R., LAZZAROTTO, A., *et al.* 2001. Inner Northern Apennines. In *Anatomy of an Orogen: The Apennines and Adjacent Mediterranean Basins.* (eds G. B. Vai & I. P. Martini), pp. 197–214. Kluwer Academy Publishers.

CASERO, P. 2004. Structural setting of petroleum exploration plays in Italy. In *Geology of Italy*. (ed U. Crescenti). Special Volume of the Italian Geological Society for the IGC 32 Florence, 189–200.

CENTAMORE, E., CHIOCCHINI, U. & MICARELLI, A. 1977. Analisi dell'evoluzione tettonico-sedimentaria dei 'bacini minori' torbiditici del Miocene medio-superiore nell'Appennino Umbro-Marchigiano e Laziale- Abruzzese. 3) Le arenarie di M. Vicino, un modello di conoide sottomarina affogata (Marche Settentrionale). *Studi Geologici Camerti* **3**, 7–56.

CHIARABBA, C., DE GORI, P., IMPROTA, L., PIO LUCENTE, F., MORETTI, M., GOVONI, A., DI BONA, M. MARGHERITI, L., MARCHETTI, A., NARDI, A. 2014. Frontal compression along the Apennines thrust system: The Emilia 2012 example from seismicity to crustal structure. *Journal of Geodynamics* **82**, 98–109.

CHIARALUCE, L., DI STEFANO, R., TINTI, E., SCOGNAMIGLIO, L., MICHELE, M., CASAROTTI, E., CATTANEO, M., DE GORI, P., CHIARABBA, C., MONACHESI, G. *et al.* 2017. The 2016 central Italy seismic sequence. A first look at the mainshocks, aftershocks, and source models. *Seismol. Res. Lett.* **88**(3), 757–771.

COOPER, M. A., GARTON, M. R., & HOSSACK, J. R. 1983. The origin of the Basse Normandie duplex, Boulonnais, France. *Journal of Structural Geology* **5**, 139–152.

COSTA, E., DI GIULIO, A., NEGRI, A. & PLESI G. 1991. *CROP 03.* Settore compreso tra Castiglion Fiorentino e Bocca Trabaria: nuovi dati stratigrafici, petrografici e strutturali. *Studi Geologici Camerti*, *Special Volume* **1**, 217–234.

COSTA, E., DI GIULIO, A., PLESI, G., VILLA, G., & BALDINI, C. 1997. Nuovi dati biostratigrafici e petrografici sulle torbiditi d'avanfossa lungo la trasversale Toscana meridionale-Protomagno. *Atti Ticin. Sc. Terra* **39**, 281–302.

CRUCIANI, F., BARCHI, M. R., KOYI, H.A. & PORRECA, M. 2017. Kinematic evolution of a regional-scale gravity-driven deep-water fold-and-thrust-belt. The Lamu Basin case-history (East Africa). *Tectonophysics* **712–713**, 30–44.

CYR, A. & GRANGER, D. 2008. Dynamic equilibrium among erosion, river incision, and coastal uplift in the northern and central Apennines, Italy. *Geology* **36**(2), 103–106.

D'AGOSTINO, N., JACKSON, J.A., DRAMIS, F. & FUNICIELLO, R. 2001. Interactions between mantle upwelling, drainage evolution and active normal faulting: an example from the central Apennines (Italy). *Geophys. J. Int.* **147**, 475–497.

D'OFFIZI, S., MINELLI, G,. & PIALLI, G. 1994. Foredeeps and thrust systems in the Northern Apennines. *Boll. Geof. Terror. e Appl.* **36**, 141–144.

DAHLEN, F. 1990. Critical taper model of fold-and-thrust belts and accretionary wedges. *Annu. Rev. Earth Planet. Sci.* **18**, 55–99.

DAMIANI, A.V., MINELLI, G. & G. PIALLI, 1991. L' unità Falterona-Trasimeno nell' area compresa fra la Val di Chiana e la Val Tiberina: sezione Terontola-Abbazia di Cassiano. In *Studi preliminari all'acquisizione de1 profile CROP 03 Punta Ala-Gabicce* (eds G. Pialli, M. R., Barchi & M. Menichetti), pp. 235–241. Stud. Geol. Camerti **l**.

DAVIS, D., SUPPE, J. & DAHLEN, F. 1983. Mechanics of fold-and-thrust belts and accretionary wedges. J. *Geophys. Res.* **88**, 1153–1172.

DE FEYTER, A.J. 1991. Gravity tectonics and sedimentation of the Montefeltro, Italy. Published Doctoral dissertation, Faculteit Aardwetenschappen der Rijksuniversiteit Utrecht.

DELLE ROSE, M., GUERRA, F., RENZULLI, A., RAVASZ-BARANYAI, L. & SERRANO F. 1994. Stratigrafia e petrografia delle Marne di Vicchio (Unità Tettonica cervarola) dell'Alta Val Tiberina (Apennino Tosco-Romagnolo). *Boll. Soc. Geol. It.* **113**, 675–708.

DEVOTI, R., D'AGOSTINO, N., SERPELLONI, E., PIETRANTONIO, G., RIGUZZI, F., AVALLONE, A., CAVALIERE, A., CHELONI, D., CECERE, G., D'AMBROSIO, C., FALCO, L., SELVAGGI, G., MÉTOIS, M., ESPOSITO, A., SEPE, V., GALVANI, A., ANZIDEI, M. 2017. A Combined Velocity Field of the Mediterranean Region. *Annals of Geophysics* **60**(2), S0217.

DOGLIONI, C., GUEGUEN, E., HARABAGLIA P., & MONGELLI, F. 1999. On the origin of west-directed subduction zones and applications to the western Mediterranean. In *The Mediterranean Basins: Tertiary Extension within the Alpine Orogen* (eds B. Durand, L. Jolivet, F. Horvath, & M. Séranne), pp. 541–561. Geological Society of London, Special Publication no. 156.

FITZ-DIAZ, E., HUDLESTON, P., TOLSON, G. 2011. Comparison of tectonic styles in the Mexican and Canadian Rocky Mountain Fold-Thrust Belt. In *Kinematic evolution and Structural styles of Fold-and-Thrust Belts* (eds J. Poblet & R.J. Lisle), pp. 149–167. Geological Society of London, Special Publication no. 349.

GASPERINI, L., BARCHI, M. R., BELLUCCI, L. G., BORTOLUZZI, G., LIGI, M., PAUSELLI, C. 2010. Tectonostratigraphy of Lake Trasimeno (Italy) and the geological evolution of the Northern Apennines. *Tectonophysics* **492**(1-4), 164–174.

GHISETTI, F. C., BARNES, P. M., ELLIS, S., PLAZA-FAVEROLA, A. A., & BARKER, D. H. N. 2016. The last 2 Myr of accretionary wedge construction in the central Hikurangi margin (North Island, New Zealand): Insights from structural modeling. *Geochem. Geophys. Geosyst.* **17**, 2661–2686.

GUNDERSON, K. L., ANASTASIO, D. J., PAZZAGLIA, F. J., & PICOTTI, V., 2013. Fault slip rate variability on 10(4)–10(5) yr timescales for the Salsomaggiore blind thrust fault, Northern Apennines, Italy, Tectonophysics **608**, 356–365.

HSÜ, K. J., CITA M. B. & RYAN, W. B. F. 1972. *I.C.R. DSDP, Initial Reports of the Deep Sea Drilling Project*. U.S. Government printing office, Washington DC, **13**, 1020.

HUNSTAD, I., SELVAGGI, G., D'AGOSTINO, N., ENGLAND, P., CLARKE P. & PIEROZZI M. 2003. Geodetic strain in peninsular Italy between 1875 and 2001. *Geophysical research letters* **30**(4), 1181.

JOLIVET, L., FACCENNA, C., GOFFÉ, B., MATTEI, M., ROSSETTI, F., BRUNET, C., FABRIZIO, S., FUNICIELLO, R., CADET, J. P., D'AGOSTINO, N., PARRA, T. 1998. Midcrustal shear zones in postorogenic extension: example from the northern Tyrrhenian Sea. *Journal of Geophysical Research: Solid Earth* **103**(B6), 12123–12160.

KING, R., & MORLEY, C. K. 2017. Wedge Geometry and Décollement Strength in Deepwater Fold-Thrust Belts. *Earth-Science Reviews* **165**, 268–279.

KOYI, H. A., 1995. Mode of internal deformation in sand wedges. *J. Struct. Geol*. **17**(2), 293–300.

KOYI, H. A., SANS, M., TEIXELL, A., COTTON, J., & ZEYEN, H. 2003. The significance of penetrative strain in the restoration of shortened layers - Insights from sand models and the Spanish Pyrenees. In *Thrust tectonics and hydrocarbon systems* (ed. K.R. McClay). AAPG Memoir **82**, 1–16.

KRUEGER, A., & GILBERT, E. 2009. Deepwater fold-thrust belts: Not all the beasts are equal. *AAPG Search and Discovery Article* #30085.

LAVECCHIA G., BROZZETTI, F., BARCHI, M. R., KELLER J. V. A. & MENICHETTI, M. 1994. Seismotectonic zoning in east-central Italy deduced from an analysis of the Neogene to Present deformations and related stress fields. *Bull. Soc. Geol. Am.* **106**, 1107–1120.

LAVECCHIA, G., BONCIO, P., CREATI, N., BROZZETTI, F. 2003. Some Aspects of The Italian Geology Not Fitting With A Subduction Scenario. *Journal of the Virtual Explorer*, **10**, 1–14.

LENA, G., BARCHI, M. R., ALVAREZ, W., FELICI, F., MINELLI, G., 2014. Mesostructural analysis of S-C fabrics in a shallow shear zone of the Umbria–Marche Apennines (Central Italy). In *Rock Deformation from Field, Experiments and Theory: A Volume in Honour of Ernie Rutter* (eds D. R. Faulkner, E. Mariani, & J. Mecklenburgh), Geological Society of London, Special Publication **409**, 149–166.

LUCCHETTI, L., BROZZETTI, F., NINI, C., NOCCHI, M. & RETTORI, R. 2002. Lithostratigraphy, integrated biostratigraphy and paleoenvironmental analysis of the Miocene Monte Santa Maria Tiberina succession (Umbria – central Italy). *Boll. Soc. Geol. It., Special Volume* **1**, 589–602.

MAESANO, F. E., TOSCANI, G., BURRATO, P., MIRABELLA, F., D'AMBROGI, C., BASILI, R., 2013. Deriving thrust fault slip rates from geological modeling: examples from the Marche coastal and offshore contraction belt, Northern Apennines, Italy. Mar. Pet. Geol. **42**, 122–134.

MAESANO, F. E., D'AMBROGI, C., BURRATO, P., TOSCANI, G., 2015. Slip-rates of blind thrusts in slow deforming areas: examples from the Po Plain (Italy). Tectonophysics **643**, 8–25.

MAESTRELLI, D., BENVENUTI, M., BONINI, M., CARNICELLI, S., PICCARDI, L., SANI, F., 2018. The structural hinge of a chain-foreland basin: Quaternary activity of the Pede-Apennine Thrust front (Northern Italy). Tectonophysics **723**, 117–135.

MARIANI, S., MAINIERO, M., BARCHI, M., VAN DER BORG, K., VONHOF, H., MONTANARI, A., 2007. Use of speleologic data to evaluate Holocene uplifting and tilting: an example from the Frasassi anticline (northeastern Apennines, Italy). Earth and Planetary Science Letters **257**, 313-328.

MARIOTTI, G., & DOGLIONI, C. 2000. The dip of the foreland monocline in the Alp sand Apennines. *Earth Planet. Sci. Lett.* **181**, 191–202.

MARTELLI, L., SANTULIN, M., SANI, F., TAMARO, A., BONINI, M., REBEZ, A., CORTI, G., SLEJKO, D. 2017. Seismic hazard of the Northern Apennines based on 3Dseismic sources. *J. Seismol.* **21**(5), 1251–1275.

MARTINIS, B., & PIERI, M. 1964. Alcune notizie sulla formazione evaporitica dell'Italia centrale e meridionale. *Mem. Soc. Geol. Ital.* **4**, 649–678.

MAZZOLI, S., BARKHAM, S., CELLO, G., GAMBINI, R., MATTIONI, L., SHINER, P., & TONDI, E. 2001. Reconstruction of continental margin architecture deformed by the contraction of the Lagonegro Basin, southern Apennines, Italy. *J Geol. Soc.* **158**, 309–319.

MCNAUGHT, M.A., & MITRA, G. 1996. The use of finite strain data in constructing a retrodeformable cross-section of the Meade thrust sheet, southeastern Idaho, U.S.A. *Journal of Structural Geology* **18**(5), 573–583.

MENEGHINI, F., BOTTI, F., ALDEGA, L., BOSCHI, C., CORRADO, S., MARRONI, M. & PANDOLFI, L. 2012. Hot fluid pumping along shallow-level collisional thrusts: The Monte Rentella Shear Zone, Umbria Apennine, Italy. *Journal of Structural Geology* **37**, 32–52.

MENICHETTI, M. & MINELLI, G. 1991. Extensional tectonics and seismogenesis in Umbria (Central Italy) the Gubbio area. *Boll. Soc. Geol. It.* **110**, 857–880.

MERLA, G. 1951. Geologia dell'Appennino settentrionale. *Bollettino della Società Geologica Italiana* **70**, 95–382.

MINISTERO DELLO SVILUPPO ECONOMICO, DGS-UNMIG, Società Geologica Italiana, Assomineraria. *Progetto Videpi*. http://unmig.sviluppoeconomico.gov.it/videpi/pozzi/dettaglio.asp?cod=4851. (30/11/2018).

MIRABELLA, F., CIACCIO, M.G., BARCHI, M. R. & MERLINI, S. 2004. The Gubbio normal fault (Central Italy): geometry, displacement distribution and tectonic evolution. *J. Struct. Geol.* **26**, 2233–2249.

MIRABELLA, F., BARCHI, M. R., LUPATELLI, A., STUCCHI E., & CIACCIO, M. G. 2008. Insights of the seismogenic layer thickness from the upper crust structure of the Umbria-Marche Apennines (central Italy). *Tectonics* **27**, TC1010.

MIRABELLA, F., BROZZETTI, F., LUPATTELLI, A., & BARCHI, M. R. 2011. Tectonic evolution of a low-angle extensional fault system from restored cross-sections in the Northern Apennines (Italy). *Tectonics* **30**, TC6002.

MITRA, G., 1994. Strain variation in thrust sheets across the Sevier fold-and-thrust belt (Idaho-Utah-Wyoming): implications for section restoration and wedge taper evolution. *Journal of Structural Geology* **6**, 51–61.

MOLLI, G. 2008. Northern Apennine–Corsica orogenic system: an updated overview. *Geological Society of London, Special Publication* **298**(1), 413–442.

MOLLI, G., & MALAVIEILLE, J. 2011. Orogenic processes and the Corsica/Apennines geodynamic evolution: insights from Taiwan. *International Journal of Earth Sciences* **100**(5), 1207–1224.

MOLLI, G., CRISPINI, L., MALUSÀ, M., MOSCA, P., PIANA, F., FEDERICO, L. 2010. Geology of the Western Alps-Northern Apennine junction area: a regional review. *Journal of the Virtual Explorer* **36**(9).

MONACO, P., & TRECCI, T. 2014. Ichnocenoses in the Macigno turbidite basin system, Lower Miocene, Trasimeno (Umbrian Apennines, Italy). *Ital. J. Geosci. (Boll. Soc. Geol. It.)* **133**(1), 116–130.

MOORE, J. C. & SILVER, E. A. 1987. Continental margin tectonics: submarine accretionary prisms. *Review of Geophysics* **25**, 1305–1312.

MORLEY, C. K., 1986. A classification of thrust fronts. *AAPG Bulletin* **70**, 12–25.

MORLEY, C. K., KING, R., HILLIS, R., TINGAY, M., BACKE, G. 2011. Deepwater fold and thrust belt classification, tectonics, structure and hydrocarbon prospectivity: A review. *Earth-Science Reviews* **104**, 41–91.

MUTTI, E, TINTERRI, R., REMACHA, E., MAVILLA, N., ANGELLA S. & FAVA, L. 1999. An introduction to the analysis of ancient turbidite basins from an outcrop perspective. *AAPG Continuing Education Course*, Note Series #39, Tulsa, OK, 61 pp.

NOCCHI, M. 1961. Sui rapporti fra la serie toscana e la serie umbra a sud di M. Acuto e di M. Filoncio (Perugia). *Boll. Soc. Geol. It.* **80**, 181–246.

NOCCHI, M. 1962. Osservazioni stratigrafiche a Nord e ad Est del Lago Trasimeno. *Mem. Soc. Geol. It.* **3**.

ORI, G. G., ROVERI M., AND VANNONI, F. 1986. Plio-Pleistocene sedimentation in the Apenninic-Adriatic foredeep (Central Adriatic Sea, Italy). In *Foreland Basins* (eds P. A. Allen, P. Homewood), pp. 183–198. IAS Special Publication no. 8.

PIALLI, G., PLESI, G., BOSCHERINI, A., MARTINI, E., DAMIANI, A. V., NOCCHI, M., LUCCHETTI, L., RETTORI, R., BUCEFALO, P. R., NEGRI, A., ARUTA, G., BIGOZZI, A., BROZZETTI, F., GALLI, M., DANIELE, G., CARDINALI, M., MERANGOLA, S., MOTTI, A., RIDOLFI, A., TOSTI, S., MENICHETTI, M. 2009. Carta geologica d'Italia: Foglio 289, Città Di Castello, scale 1:50.000. *Istituto Superiore per la Protezione e la Ricerca Ambientale,* Rome. http:// www.isprambiente.gov.it /Media

PICOTTI, V. & PAZZAGLIA, F. 2008. A new active tectonic model for the construction of the Northern Apennines mountain front near Bologna. *Journal of Geophysical Research* **113**, B08412.

PLESI, G., GALLI, M. & DANIELE, G. 2002*a*. The Monti Rognosi OphioliticUnit (cfr. Calvana Unit Auct.) paleogeographic position in the External Ligurian Domain: relationships with the tectonic units derived from the Adriatic margin. Boll. Soc. Geol. It., Vol. spec., 1, 273-284.

PLESI, G., LUCCHETTI, L., BOSCHERINI, A., BOTTI, F., BROZZETTI, F., BUCEFALO, P. R., DANIELE, G., MOTTI, A., NOCCHI, M., RETTORI, R. 2002*b*. The Tuscan succession of high Tiber Valley (F. 289, "Città di Castello"): biostratigraphic, petrographic and structural features, regional correlations. *Boll. Soc. Geol. It. Special Volume* in memory of G. Pialli, 385–436.

PLESI, G., DAMIANI, A. V., BOSCHERINI, A., MARTINI, E., LUCCHETTI, L., PALANDRI, S., RETTORI, R., TUSCANO, F., BOTTI, F., DANIELE, G., TOSTI, S., DEL GAIA, F., ARCALENI, A., GALLI, M., SABATINI, F., PREZIOSI, E., BARTOCCINI, P., UFFREDDUZZI, T. 2010. Carta geologica d'Italia: Foglio 299, Umbertide scale 1:50.000. *Istituto Superiore per la Protezione e la Ricerca Ambientale*, Rome. http:// www.isprambiente.gov.it /Media

POBLET. J., LISLE R. J. 2011. Kinematic evolution and structural styles of fold-and-thrust belts. *Geological Society of London, Special Publications* **349**, 1–24.

PONZA, A., PAZZAGLIA, F. J., PICCOTTI, V., 2010. Thrust-fold activity at the mountain front of the Northern Apennines (Italy) from quantitative landscape analysis. Geomorphology 123, 211–231.

PORRECA, M., MINELLI, G., ERCOLI, M., BROBIA, A., MANCINELLI, P., CRUCIANI, F., GIORGETTI, C., CARBONI, F., MIRABELLA, F., CAVINATO, G., CANNATA, A., PAUSELLI C., & BARCHI, M. R. 2018. Seismic Reflection Profiles and Subsurface Geology of the Area Interested by the 2016–2017 Earthquake Sequence (Central Italy). *Tectonics* **37**(4), 1116–1137.

PRICE, R. A. 1981. The Cordilleran foreland thrust and fold belt in the southern Canadian Rocky Mountains. In *Thrust and Nappe Tectonics* (eds K. R. McClay, & N. J. Price), pp. 427–448. Geological Society of London, Special Publication no. 9.

RICCI LUCCHI, F. 1986. The Oligocene to recent foreland basins of the Northern Apennines. In *Foreland Basins* (eds P. A. Allen, P. Homewood), pp. 105–139. IAS Special Publication no. 8.

RICCI LUCCHI, F. & PIALLI, G. 1973. Apporti secondari nella MA: 1. Torbiditi di conoide e di piana sottomarina a Est-Nord-Est di Perugia. Bollettino Societa Geologica Italiana 92, 669-712.

RYAN, W. B. F. & CITA, M. B. 1978. The nature and distribution of Messinian erosional surface Indication of a several kilometres-deep Mediterranean in the Miocene. *Mar. Geol.* **27**, 193–230.

SCARSELLI, S., SIMPSON, G. D. H., ALLEN, P. A., MINELLI, G., GAUDENZI, L. 2007. Association between Messinian drainage network formation and major tectonic activity in the Marche Apennines (Italy). *Terra Nova* **19**(1), 74–81.

SERPELLONI, E., ANZIDEI, M., BALDI, P., CASULA G., & GALVANI, A. 2005. Crustal velocity and strain-rate fields in Italy and surrounding regions: new results from the analysis of permanent and non-permanent GPS networks. *Geophys. J. Int.* **161**, 861–880.

SERPELLONI, E., ANZIDEI, M., BALDI, P., CASULA G., & GALVANI, A. 2006. GPS measurement of active strains across the Apennines. *Annals of geophysics*, supplement to Vol. **49**(1).

SESTINI, G. 1970. Flysch facies and turbidite sedimentology. *Sedimentary Geology* **4**, 559-597.

SIGNORINI, R., & ALIMENTI, M. 1968. La serie stratigrafica del Monte Rentella fra il Lago Trasimeno e Perugia. *Geol. Rom. VII*, 75–94.

SINCLAIR, H. D. 1997. Flysch to molasse transition in peripheral foreland basins: The role of the passive margin versus slab breakoff. Geology **25**(12), 1123–1126.

SUPPE, J. 2007. Absolute fault and crustal strength from wedge tapers. *Geology*, **35**, 1127–1130.

TESEI, T., LACROIX, B., & COLLETTINI, C., 2015. Fault strength in thin-skinned tectonic wedges across the smectite-illite transition: Constraints from friction experiments and critical tapers. *Geology*, doi:10.1130/G36978.1.

THOMSON, S. N., BRANDON, M. T., REINERS, P. W., ZATTIN, M., ISAACSON, P. J. & BALESTRIERI, M. L. 2010. Thermochronologic evidence for orogen-parallel variability in wedge kinematics during extending convergent orogenesis of the northern Apennines, Italy. *GSA Bulletin* **122**(7/8), 1160–1179.

WEGMANN, K. & PAZZAGLIA, F. 2009. Late Quaternary fluvial terraces of the Romagna and Marche Apennines, Italy: climatic, lithologic, and tectonic controls on terrace genesis in an active orogen. *Quaternary Science Reviews* **28**.